

New Fiber Materials with Sorption Capacity at 5.0 g-U/kg Adsorbent under Marine Testing Conditions

Fuel Cycle Research & Development

Prepared for
U.S. Department of Energy
Fuel Cycle Research & Development
T. Saito, S. Brown, S. Das, R. Mayes, C. Janke, S. Dai
Oak Ridge National Laboratory
L.-J. Kuo, J. Strivens, N. Schlafer, J. Wood, G. Gill
Pacific Northwest National Laboratory
M. Flicker Byers, E. Schneider
University of Texas Austin
March 30, 2016
FCRD-2016- M2FT-16OR030201031



Approved for public release.
Distribution is unlimited.

DISCLAIMER

This information was prepared as an account of work sponsored by an agency of the U.S. Government. Neither the U.S. Government nor any agency thereof, nor any of their employees, makes any warranty, expressed or implied, or assumes any legal liability or responsibility for the accuracy, completeness, or usefulness, of any information, apparatus, product, or process disclosed, or represents that its use would not infringe privately owned rights. References herein to any specific commercial product, process, or service by trade name, trade mark, manufacturer, or otherwise, does not necessarily constitute or imply its endorsement, recommendation, or favoring by the U.S. Government or any agency thereof. The views and opinions of authors expressed herein do not necessarily state or reflect those of the U.S. Government or any agency thereof.

SUMMARY

The Fuel Resources program of the Fuel Cycle Research and Development program of the Office of Nuclear Energy (NE) has focused on assuring that nuclear fuel resources are available in the United States for a long term. An immense source of uranium is seawater, which contains an estimated amount of 4.5 billion tonnes of dissolved uranium. Extraction of the uranium resource in seawater can provide a price cap and ensure centuries of uranium supply for future nuclear energy production. NE initiated a multidisciplinary program with participants from national laboratories, universities, and research institutes to enable technical breakthroughs related to uranium recovery from seawater. The goal is to develop advanced adsorbents to make the seawater uranium recovery technology a cost competitive, viable technology. Under this program, Oak Ridge National Laboratory (ORNL) has developed several novel adsorbents, which enhanced the uranium capacity 4-5 times from the state-of-the art Japanese adsorbents.

Uranium exists uniformly at a concentration of ~ 3.3 ppb in seawater. Because of the vast volume of the oceans, the total estimated amount of uranium in seawater is approximately 1000 times larger than its amount in terrestrial resources. However, due to the low concentration, a significant challenge remains for making the extraction of uranium from seawater a commercially viable alternative technology. The biggest challenge for this technology to overcome to efficiently reduce the extraction cost is to develop adsorbents with increased uranium adsorption capacity. Two major approaches were investigated for synthesizing novel adsorbents with enhanced uranium adsorption capacity. One method utilized conventional radiation induced graft polymerization (RIGP) to synthesize adsorbents on high-surface area trunk fibers and the other method utilized a chemical grafting technique, atom-transfer radical polymerization (ATRP). Both approaches have shown promising uranium extraction capacities: RIGP adsorbent achieved 5.00 ± 0.15 g U/kg-ads., while ATRP adsorbent achieved 6.56 ± 0.33 g U/kg-ads., after 56 days of seawater exposure. These achieved values are the highest adsorption capacities ever reported for uranium extraction from seawater.

Novel fiber adsorbents (AF1) comprised of acrylonitrile (AN) and itaconic acid prepared by RIGP onto high-surface-area, hollow-gear polyethylene fibers. The AF1 adsorbent was subsequently tested in natural seawater at the Pacific Northwest National Laboratory (PNNL). This report describes the preparation, characterization and testing of this novel adsorbent including results on simulated seawater testing and field adsorption testing using natural seawater. Investigation of the optimum reaction parameters for conversion of grafted cyano groups into amidoxime groups was conducted by reaction with hydroxylamine at different temperatures and time periods in a variety of water based and organic solvents. The ^{13}C CP/MAS spectra of AF1 adsorbent fibers amidoximated in 50/50 (w/w) water-methanol and in dimethyl sulfoxide (DMSO) clearly revealed that both the open-chain amidoxime and cyclic imide dioxime were formed during the course of the reaction. Formation of imide dioxime from amidoxime was found to occur slowly and gradually with increasing reaction time. Higher diffusivity of DMSO as compared to water-methanol, in the grafted trunk PE fiber resulted in faster kinetics of the amidoximation reaction and a larger amount of cyclic imide dioxime throughout the adsorbent. The uranium adsorption capacity of the amidoximated AF1 samples was determined after: (i) 24 h contact with sodium based brine spiked with uranium and (ii) 56 days exposure in natural seawater (Sequim Bay, WA) in flow-through-columns. The performance of the adsorbents after exposure in natural seawater was consistent with the laboratory screening results and the AF1 samples amidoximated in DMSO at 70 °C for 3 h resulted in the highest uranium adsorption capacity (5.00 ± 0.15 g U/kg-ads) with much faster adsorption kinetics compared to AF1 adsorbent amidoximated in water-methanol solution.

The other novel fiber adsorbents were prepared by ATRP of 2-hydroxyethyl acrylate and acrylonitrile. The composition of grafted chain, i.e., varied comonomer ratio in simultaneous grafting with AN, had a significant impact on the uranium adsorption capacity, indicating the optimum reaction conditions to prepare high-performance fiber adsorbents. The optimized ATRP adsorbent achieved 6.56 ± 0.33 g U/kg-

ads., after 56 days of seawater exposure. With this capacity, the estimated uranium production cost ranges from \$420-860/kg or \$370-760/kg depending on the assumptions. These values are so far the best cost estimates reported. In the case of a constant 5% adsorbent degradation rate, the optimal soaking campaign is around 50 days, while the worst case degradation optimizes closer to 10 days of exposure. The cost decrease, roughly 10%, is predominantly a result of the improvement in adsorbent capacity, as this has been previously identified as one of the most significant cost drivers.

The study successfully demonstrated new fiber materials with sorption capacity at 5.0 g-U/kg adsorbent under marine testing conditions. Further optimization, investigation of other new materials as well as deepening our understanding will develop adsorbents that have even higher uranium adsorption capacity, increased selectivity, and faster kinetics.

CONTENTS

SUMMARY	iii
1. Introduction	1
2. Background Information.....	1
3. Experimental Design	3
3.1 Adsorbent Preparation	3
3.1.1 Materials and Characterization Methods	3
3.1.2 Adsorbent Synthesis	3
3.2 Capacity Evaluation.....	4
3.2.1 Simulated Seawater Screening for Uranium Adsorption Determination	4
3.3.2 Seawater tests	5
4. Results and Discussion	6
4.1 Amidoximation and Characterization of Adsorbents Prepared by RIGP.....	6
4.1.1 Performance of adsorbents for uranium adsorption	11
4.1.2 Kinetics of uranium adsorption.....	17
4.1.3 Conclusions for novel adsorbents prepared by RIGP	18
4.2 Novel Adsorbents Prepared by ATRP.....	19
4.2.1 ATRP grafting and uranium uptake in uranium-spiked brine	19
4.2.2 Characterization of adsorbent fibers prepared by ATRP.....	21
4.2.3 Uranium uptake of ATRP fiber adsorbents in seawater	22
4.2.4 Economic analysis of ATRP-based fiber adsorbents	23
4.2.5 Conclusions for novel adsorbents prepared by ATRP.....	28
Acknowledgments	28
Appendix A: References.....	29

FIGURES

Figure 1.	Schematic diagram of flow-through-column experiments using a parallel configuration at the Marine Sciences Laboratory of PNNL.	5
Figure 2.	FTIR spectra of AF1 adsorbents amidoximated with 10 wt% hydroxylamine in (A) H ₂ O, (B) CH ₃ OH, (C) 50:50 (w/w) H ₂ O- CH ₃ OH, (D) IPA, (E) DMSO, (F) 50:50 (w/w) H ₂ O-DMSO, for 1, 3, 6, and 24h.	8
Scheme 1.	Reaction mechanism of conversion of grafted polyacrylonitrile into open-chain amidoxime and cyclic imide dioxime upon treatment with hydroxylamine and heat.	9
Figure 3.	¹³ C CP/MAS spectra of grafted AF1, and AF1 amidoximated with 10 wt% hydroxylamine at room temperature (for 96h) and 80 °C (for 1, 3, 6, and 24 h) in (A) 50:50 (w/w) H ₂ O-CH ₃ OH, (B) DMSO.	10
Figure 4.	Uranium adsorption performance of AF1 adsorbent amidoximated with 10 wt% hydroxylamine in different solvents for different time periods at 80 °C: (A) after contacting with simulated seawater (spiked with uranium) for 24 h, (B) after 21 days exposure with seawater (Sequim Bay) in flow-through columns.	12
Figure 5.	Uranium adsorption performance of AF1 adsorbent after contacting with simulated seawater (spiked with uranium) for 24 h. The adsorbents were amidoximated with 10 wt% hydroxylamine at different temperatures for different time periods in solvents: (A) 50:50 (w/w) H ₂ O-CH ₃ OH and (B) DMSO.	14
Figure 6.	Uranium adsorption performance of AF1 after 21 days exposure with seawater (Sequim Bay) in flow-through columns. The adsorbents were amidoximated with 10 wt% hydroxylamine at different temperatures, for different time periods, in solvents: (A) 50:50 (w/w) H ₂ O-CH ₃ OH and (B) DMSO.	16
Figure 7.	Uranium adsorption performance of AF1 after 56-days exposure with seawater (Sequim Bay) in flow-through columns. The adsorbents were amidoximated with 10 wt% hydroxylamine in DMSO at: (A) 80 °C for different time periods and (B) 70 °C for 3 h.	17
Figure 8.	(A) Adsorption kinetics of uranium by the AF1 adsorbents after 56 days contact with seawater in flow-through columns.	18
Figure 9.	Synthesis steps of uranium adsorbent fibers from PVC-co-CPVC fibers.	19
Figure 10.	Uranium uptake in 750-mL U-spiked brine (Different grafted fibers, AO'd at 80 °C for 2 days followed by 1 day, varied KOH treatment at 80 °C).	21
Figure 11.	100 MHz ¹³ C CP/MAS NMR spectra of fibers as (a) grafted (fiber A3), (b) amidoximated (2 d then 1 d at 80 °C), and (c) KOH-treated (3.5 h at 80 °C). Asterisk (*) denotes spinning sideband (spinning speed = 8.0 kHz).	22
Figure 12.	Kinetic plots of uranium and vanadium uptake of two batches of fiber A3 in Sequim Bay, WA, with one-site ligand saturation modeling (salinity normalized to 35 psu).	23
Figure 13.	Process flow diagram for adsorbent production via ATRP.	24
Figure 14.	Uranium production cost for case 1 as a function of number of adsorbent uses.	25
Figure 15.	Breakdown of adsorbent production operating and maintenance cost.	26
Figure 16.	Uranium production cost as a function of number of adsorbent uses for case 2.	27
Figure 17.	Comparison of cost breakdown for cases 1 and 2.	28

TABLES

Table 1.	ATRP of AN and uranium uptake in 750-mL U-spiked brine.....	20
Table 2.	Simultaneous copolymerization of AN and HEA.....	20
Table 3.	Uranium uptake in seawater at Sequim bay, WA.....	22
Table 4.	Uranium adsorption capacity from one-site ligand saturation modeling.....	23
Table 5.	Price for bulk orders of chemical inputs.....	24
Table 6.	Base case parameters.....	25

1. INTRODUCTION

The current mission of the Fuel Resources subprogram of the Fuel Cycle Research and Development program of the DOE Office of Nuclear Energy (NE) is to identify and implement actions to assure that economic nuclear fuel resources remain available in the United States. Seawater contains more than 4 billion tonnes of dissolved uranium at a concentration of 3.3 ppb. Combined with a suitable extraction cost, this unconventional seawater resource can potentially provide a price cap and ensure centuries of uranium supply even with aggressive world-wide growth in nuclear energy applications.

NE-5 initiated a multidisciplinary team from national laboratories, universities, and research institutes in 2011. The team seeks to take advantage of recent developments in (1) high performance computing, (2) advanced characterization instruments, and (3) nanoscience and nanomanufacturing technology to enable technical breakthroughs related to uranium recovery from seawater. The program goal is to develop advanced adsorbent materials to reduce the seawater uranium recovery technology cost and uncertainties. The R&D investment strategy is focused on developing advanced adsorbents that can simultaneously enhance uranium adsorption capacity, selectivity, kinetics, and materials durability. As a result of this investment strategy, Oak Ridge National Laboratory (ORNL) has developed novel amidoxime-based adsorbents, which enhanced the uranium capacity for 4-5 times of leading Japanese adsorbents that were proven in field marine testing.

Previous studies under this program demonstrated novel amidoxime-based adsorbent of high surface area prepared by conventional radiation-induced graft polymerization (RIGP) that tripled the uranium capacity of leading Japanese adsorbents. This milestone further investigated the optimization of the adsorbent preparation conditions via RIGP and atom transfer radical polymerization (ATRP), a chemical grafting technique. Both approaches have shown promising uranium extraction capacities: RIGP adsorbent achieved 5.00 ± 0.15 g U/kg-ads., while ATRP adsorbent achieved 6.56 ± 0.33 g U/kg-ads., after 56 days of seawater exposure. These achieved values are the best adsorption capacities ever reported and 4-5 times higher than the capacity of leading Japanese adsorbents. This work has been concluded and the results have been compiled in this milestone report.

2. BACKGROUND INFORMATION

A 2011 study by the Organization for Economic Co-operation and Development estimated that, at the current consumption rate, the global conventional reserves of uranium (7.1 million tonnes) could be depleted in roughly a century. Therefore, it is of significant interest to look for resources of uranium other than the conventional terrestrial uranium ores¹. Uranium (U) exists uniformly as uranyl carbonates (primarily as $[\text{UO}_2(\text{CO}_3)_3]^{4-}$) at a concentration of ~ 3.3 ppb in seawater. Because of the vast volume of the oceans, uranium in seawater amounts to 4.5×10^9 tonnes, approximately 1000 times larger than the terrestrial resources.² The readily accessible reserves of uranium in conventional terrestrial mining will eventually deplete, and scarcity of uranium as well as higher cost to mine lower grade deposits might become a significant issue in the future, even for currently operating nuclear plants. Moreover, the environmental and human health impact for the conventional terrestrial mining is always a big concern. To resolve these issues associated with the conventional terrestrial mining of uranium, the extraction of uranium from seawater presents a very attractive alternative route to obtain uranium for nuclear fuel needs. The biggest challenge for making the extraction of uranium from seawater a commercially viable alternative technology is the development of adsorbents with increased uranium adsorption capacity.³ A recent estimate of a polymer adsorbent for uranium recovery from seawater indicated that a polymer fiber adsorbent with 6 g/kg uranium adsorption capacity at 3% capacity loss per use with 10 recycling uses or

30 g/kg uranium adsorption capacity at single use would result in \$290/kg-uranium, a comparable uranium price to that (\$100-335/kg-uranium) from conventional terrestrial resources³. The most significant way to achieve a competitive uranium extraction cost compared with conventional terrestrial mining is by increasing the uranium adsorbent capacity in seawater extraction. The adsorbents need to be carefully designed to achieve significant enhancement on the extraction efficiency of uranium from seawater, especially as this technology requires a highly selective extraction from such a low concentration of uranium in seawater.

During this Fuel Cycle Research and Development program, ORNL adsorbents have demonstrated a three-fold enhancement in uranium adsorption capacity by polyamidoxime (PAO)-based adsorbents prepared with relatively high surface area polyethylene (PE) fibers.⁴ In this report, the two major approaches were investigated for synthesizing novel adsorbents with enhanced uranium adsorption capacities. One method utilized conventional RIGP to synthesize adsorbents on high-surface area trunk fibers and the other method utilized ATRP. The synthesis protocol of the RIGP method was further optimized to enhance the uranium adsorption capacity from the previously achieved three-fold enhancement. The ATRP method was used to investigate various trunk materials, comonomers, and optimized reaction conditions for producing high-capacity uranium adsorbents.

A new adsorbent (AF1) was synthesized at the ORNL by RIGP of acrylonitrile (AN) monomer and itaconic acid (ITA) co-monomer onto high surface area polyethylene fibers. Two important steps, (1) amidoximation (i.e., conversion of polyacrylonitrile (PAN) into PAO by reaction with hydroxylamine) and (2) alkaline conditioning of PAO, are necessary to prepare the adsorbent for uranium uptake. Systematic optimization of this process has been proven effective in improving the adsorbent performance for uranium extraction from seawater, in terms of adsorption capacity, adsorption rate, process cost etc. Thus, this study reports a systematic investigation on the effects of different amidoximation parameters such as reaction time, reaction temperature, and the use of different kinds of solvents, on uranium extraction from seawater.

Our recent efforts have also been focusing on utilizing controlled radical polymerization, especially ATRP, to graft uranium-adsorbing polymer chains to fiber substrates. In comparison to lack of tunability in conventional RIGP, the use of a controlled radical polymerization method offers several advantages including more controllable composition and controllable degree of polymerization (length of graft chains), which ATRP can either increase to a much higher degree of grafting (d.g.) or prepare the exact d.g. for the best performance. While ATRP can be utilized in various substrates^{2b}, grafting onto polymeric fibers for uranium adsorption has several advantages: 1) already proven to be deployable in seawater,⁵ 2) light weight, 3) easy to fabricate to various shapes and lengths. In a previous report⁶, we utilized a hybrid approach of using RIGP and ATRP to prepare polymeric fiber adsorbents for uranium recovery from seawater. That study demonstrated the feasibility of using ATRP as a synthesis method. The uranium adsorption capacity after 56-days seawater exposure was moderate (3.02 g U/kg-ads.). More recently, further advancements were made for fiber adsorbents prepared via ATRP. To eliminate the RIGP step, the new class of trunk fibers was prepared by the chlorination of PP round fiber, hollow-gear-shaped PP fiber, and hollow-gear-shaped PE fiber as well as using commercially available poly(vinyl chloride)-*co*-chlorinated poly(vinyl chloride) (PVC-*co*-CPVC) fiber.⁷ ATRP of AN and *tert*-butyl acrylate (*t*BA) from the halide-functionalized trunk fibers was successfully performed and degrees of grafting (d.g.) as high as 2570% were obtained. The resulting adsorbent fibers showed uranium adsorption capacities significantly higher than the JAEA reference fiber in natural seawater tests (2.42–3.24 g/kg in 42 days of seawater exposure and 5.22 g/kg in 49 days of seawater exposure; JAEA: 1.66 g/kg in 42 days of seawater exposure and 1.71 g/kg in 49 days of seawater exposure). However, due to incomplete hydrolysis of *t*BA as well as a sensitive monomer reactivity during polymerization, the results were inconsistent. Therefore, this study focused on the role of hydrophilicity-controlling comonomer, namely 2-hydroxyethyl

methacrylate (HEMA) and 2-hydroxyethyl acrylate (HEA). By changing the comonomer in simultaneous grafting with AN, both the uranium adsorption capacity and the reproducibility in environmental seawater were significantly increased.

3. EXPERIMENTAL DESIGN

Two types of novel fiber adsorbents have been prepared via two very different techniques, RIGP and ATRP. Multiple chemical and physical characterization techniques have been employed to strengthen the conclusions related to the adsorbent performance for each parameter investigated. Experiments of uranium uptake from seawater for this study have been performed at the Marine Sciences Laboratory of PNNL. The structure-property relationships of the novel adsorbents, in terms of performance with seawater, are described below.

3.1 Adsorbent Preparation

3.1.1 Materials and Characterization Methods

All chemicals were reagent-grade or higher. Acrylonitrile (AN), itaconic acid (ITA), tetrahydrofuran (THF), methanol, dimethylsulfoxide (DMSO), iso-propanol (IPA), hydroxylamine hydrochloride (HA-HCl) and potassium hydroxide (KOH) were obtained from Sigma-Aldrich. Ultrapure water (18 M Ω cm⁻¹, Thermo scientific Nanopore) was used in the preparation of HA-HCl and KOH solutions. High-surface-area polyethylene fibers (PE, hollow-gear) were prepared by bicomponent melt-spinning at Hills, Inc. (Melbourne, FL), using polylactic acid (PLA) as the co-extrusion polymer. Reagents used to prepare the sodium-based brine solution are uranyl nitrate hexahydrate (UO₂(NO₃)₂·6H₂O, B&A Quality), sodium bicarbonate (NaHCO₃, ACS Reagent, Aldrich) and sodium chloride (>99%, Aldrich). A 1000 ppm uranium (U) standard solution (High Purity Standards, North Charleston, USA) was used to prepare the ICP standards. The PVC-co-CPVC fiber used in this study was Rhovyl™'s ZCS tow fiber provided by Whitin Yarns and Fibers (Westport, MA). Acrylonitrile (AN, 99+%, Acros) and 2-hydroxyethyl acrylate (HEA, 97%, Acros) were passed through an activated alumina column prior to use. Copper(II) chloride (CuCl₂, ≥99.995%, Aldrich), copper(I) chloride (CuCl, 99.999%, Alfa), tris(2-(dimethylamino)ethyl)amine (Me₆TREN, 99+%, Alfa), ethylene carbonate (EC, 99+%, Acros), dimethyl sulfoxide (DMSO, 99.95%, Fisher), methanol (99.9%, Fisher), and potassium hydroxide (88.4%, Fisher) were used as received. Hydroxylamine solution (HA, 50 wt % in water, Aldrich) was used during the amidoximation. Deionized water was freshly collected prior to the usage from a Milli-Q Gradient water deionizer. Elemental analyses (EA) for C, H, N, O, and Cl were performed by Galbraith Laboratories, Inc. (Knoxville TN). Solid-state ¹³C CP/MAS (cross-polarization/magic-angle spinning) NMR spectra were acquired on a Varian Inova 400 MHz spectrometer and referenced to an external standard, hexamethylbenzene, at 17.17 ppm. Fourier transform infrared (FTIR) spectra were acquired on an Excalibur FTIR with an MVP-Pro ATR Accessory. Scanning electron microscopy (SEM) imaging was performed on the Zeiss Auriga microscope with an electron beam operation of 3keV, which is a dual beam FIB (Focused Ion Beam) with a field emission electron column for high resolution electron imaging and a Canion Ga⁺ column for precision ion beam milling.

3.1.2 Adsorbent Synthesis

Radiation-induced Graft Polymerization (RIGP)

The adsorbent fibers were prepared by RIGP at the NEO Beam Electron Beam Cross-linking Facility (Middlefield, OH). Prior to irradiation, the co-extruded polylactic acid (PLA) was removed from the fibers by treating with excess THF at 65-70 °C, followed by drying at 40 °C under vacuum. The pre-

weighed dry fiber samples, sealed inside double-layered plastic bags under nitrogen were irradiated with the electron beam to a dose of approximately 200 ± 10 kGy using 4.4-4.8 MeV electrons and 1 mA current from an RDI Dynamitron electron beam machine. The irradiated fibers were immediately immersed in a 300-mL flask containing previously de-gassed grafting solutions consisting of AN and ITA in DMSO, and placed in an oven at 64 °C for grafting. After 18 h of grafting, the fibers were washed with DMF to remove unreacted monomers and homopolymers followed by rinsing with methanol and dried at 40 °C under vacuum.

Atom-Transfer Radical Polymerization

First, $\text{CuCl}_2 \cdot 2\text{H}_2\text{O}$ (3.3 mg, 1.9×10^{-5} mol), PVC-co-CPVC fiber (150 mg, 2.08×10^{-3} mol vinyl chloride repeating units), EC (40.6 mL, 50 vol %), HEA (varied, e.g., 17.2 g, 0.144 mol, for 375 HEA:500 AN in feed), AN (varied, e.g., 10.3 g, 0.192 mol, for 375 HEA:500 AN in feed, and Me_6TREN (106 mg, 4.55×10^{-4} mol) were added to a Schlenk flask equipped with a magnetic stirring bar. The flask was subjected to three freeze-pump-thaw (FPT) cycles. Then, CuCl (38.0 mg, 3.84×10^{-4} mol) was added to the flask, under an argon flow, while the contents were at a solid state. The reaction mixture was subjected to another FPT cycle. The flask was placed in an oil bath with the temperature equilibrated at 65 °C, and the reaction was pursued under a sealed argon atmosphere for 24 h. The reaction was terminated by exposure to air. The fiber product was washed with DMSO until the supernatant was colorless, rinsed three times with methanol, and dried under vacuum at 40 °C overnight or longer, until constant weights were obtained. Degrees of grafting were calculated from: $100 \times \text{weight increase from grafting} / \text{weight of PVC-co-CPVC fiber}$. The d.g. values presented in subsequent tables are averaged values from at least four repeated experiments.

Amidoximation of grafted AN

The AN grafted PE fibers (AF1 hereafter) were treated with 10 wt % hydroxylamine hydrochloride neutralized with KOH, for conversion into amidoxime (AO) groups. The hydroxylamine solution was prepared using a variety of solvents, such as de-ionized water, methanol, IPA, DMSO, 50/50 (w/w) water-methanol, 50/50 (w/w) water-IPA, 20/80 (w/w) water-THF, 50/50 (w/w) water-THF and 50/50 (w/w) water-DMSO. The amidoximation of AF1 with different hydroxylamine solutions was carried out at different temperatures (i.e., 60, 65, 70, 75, and 80 °C) for different periods of time (i.e., 1, 3, 6, 24 h), while amidoximation of PVC-co-CPVC-g-(PAN-co-PHEA) with 50/50 (w/w) water-methanol was performed twice over long reaction periods (i.e., 2 d, followed by 1 d). The samples were then washed under vacuum filtration with deionized water followed by drying at 40 °C under vacuum.

KOH conditioning

The amidoximated AF1 adsorbents were conditioned with 0.44M KOH at 80 °C for 1 h or 3 h prior to exposing them in simulated seawater screening solution as well as real seawater for determining the uranium uptake capacity.

3.2 Capacity Evaluation

3.2.1 Simulated seawater screening for uranium adsorption determination

Batch experiments with synthetic seawater were conducted at the University of Tennessee. The sodium-based brine solution used for screening consists of 193 ppm sodium bicarbonate, 25,600 ppm sodium chloride, and 8 ppm uranium from uranyl nitrate hexahydrate in $18.2 \text{ M}\Omega \text{ cm}^{-1}$ water. The pH of the test solution was 7.8 ± 0.2 . The concentrations of sodium, chloride and bicarbonate ions were similar to those found in seawater. A sample of the solution was collected prior to the addition of adsorbent to determine the initial uranium concentration. Each of the KOH-conditioned AF1 samples (~15 mg) was then

contacted with 750 mL of simulated seawater solution for 24 hours at room temperature with constant shaking at 400 rpm. After 24 hours of shaking, an aliquot was taken and the initial and final solutions were analyzed using inductively coupled plasma-optical emission spectroscopy (Perkin Elmer Optima 2100DV ICP-OES). The uranium adsorption capacity was determined from the difference in uranium concentration in the solutions, using Eq 1. The ICP-OES was calibrated using six standard uranium solutions with concentrations ranging from 0-10 ppm, which were prepared from 1000 ppm uranium in 5 wt % nitric acid stock solution, and a linear calibration curve was obtained. A blank solution of 2–3 wt % nitric acid was also prepared and washouts were monitored between samples to ensure no uranium was carried over into the next analysis. In addition, a solution of 5 ppm yttrium in 2 wt % nitric acid was used as an internal standard, which was prepared from 1000 ppm stock solution (High-Purity Standards, North Charleston, USA).

$$\text{Uranium (U) adsorption capacity} = \left[\frac{\text{Initial [U]} \left(\frac{\text{mg}}{\text{L}} \right) - \text{Final [U]} \left(\frac{\text{mg}}{\text{L}} \right)}{\text{g of dry adsorbent}} \right] \times (\text{Soln. vol.}) (\text{L}) \quad (1)$$

3.2.2 Seawater tests

The uranium adsorption kinetics and the uranium adsorption capacities for the adsorbents were carried out at the Marine Sciences Laboratory, Pacific Northwest National Laboratory (PNNL) for 0-56 days in flow-through columns using natural seawater (Figure 1). The quality of seawater was quantitatively monitored for pH, temperature, salinity, and trace-metal concentrations over the whole exposure period. A schematic diagram of the flow-through-column test is shown in Figure 1. Marine testing was performed using filtered (0.45 μm) seawater at a temperature of 20 ± 2 °C and at a flow rate of 250 mL/min, using an active pumping system. Glass wool and glass beads were used as packing materials in the columns.

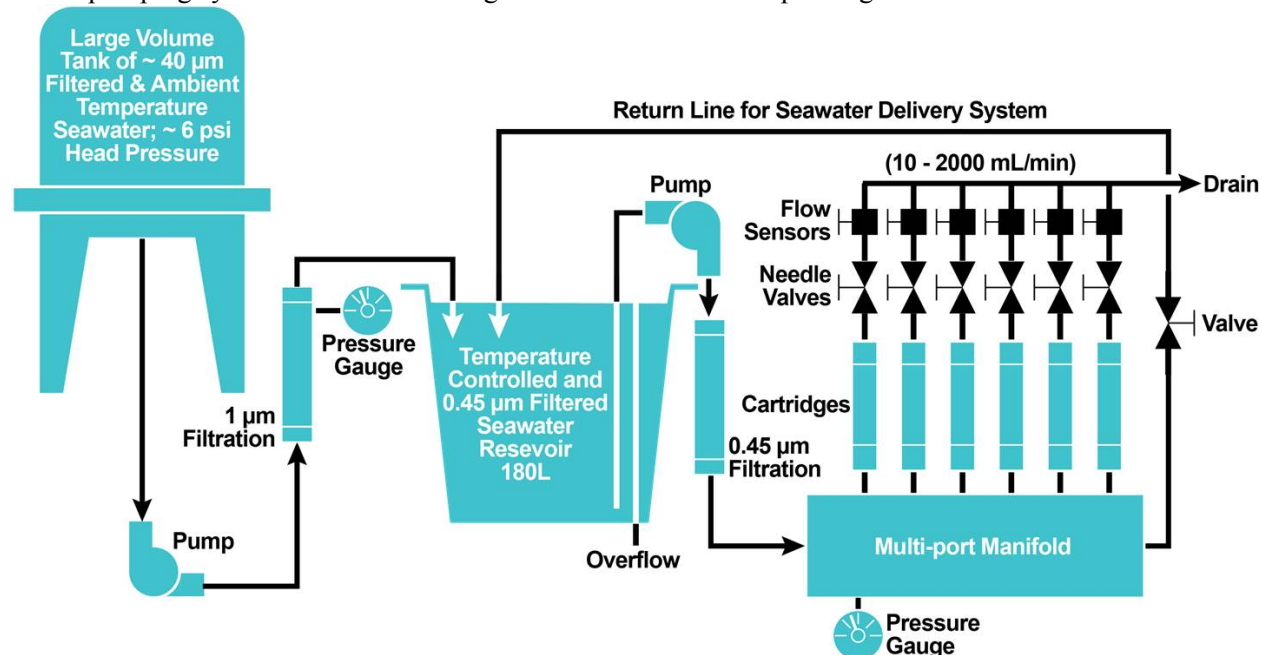


Figure 1. Schematic diagram of flow-through-column experiments using a parallel configuration at the Marine Sciences Laboratory of PNNL.

Sample Handling and Analytical Procedures at PNNL

The AF1 adsorbents (~50 mg each) were conditioned with 0.44 M KOH at 80°C for 1 h. The conditioned adsorbents were packed into columns (1" diameter, 6" long) fabricated from all plastic components,

mostly polyvinylchloride (PVC) and polypropylene. Pre-cleaned glass wool and 5 mm glass beads were used to hold the adsorbents in place in the column. Ambient seawater was pumped from Sequim Bay, WA and filtered through 0.45 μm polypropylene cartridges for the continuous-flow adsorption experiment. The temperature of the incoming seawater was maintained at 20 ± 1 $^{\circ}\text{C}$ using an all-titanium immersion-heater. The flow rate of seawater in each column was controlled at 250-300 $\text{mL}\cdot\text{min}^{-1}$. Temperatures and flow rates were monitored at 10 min intervals using a temperature logger equipped with a flexible hermetically sealed RTD sensor probe (OMEGA Engineering, Stamford, CT, USA) and an in-line turbine-style flow sensor (Model DFS-2W, Digiflow Systems), respectively. During the course of the flow-through adsorption experiments, seawater salinity and pH were monitored daily using a hand-held salinometer (Model 30, YSI) and pH meter (Orion 3 STAR, Thermo). After certain (e.g. 56) days of seawater exposure in the columns was completed, the adsorbents were removed from the columns and desalted by thoroughly rinsing with de-ionized water. The adsorbents were further dried using a heating block and weighed. The adsorbents loaded with metal ions were digested with a 50% aqua regia solution at 85 $^{\circ}\text{C}$ for 3 hours. Samples were further diluted with de-ionized water in order to be in the desired concentration range before analysis. Analysis of uranium and other trace elements in the digested solutions was carried out using a Perkin-Elmer Optima 4300DV inductively coupled plasma optical emission spectrometer (ICP-OES), with quantification based on standard calibration curves.

4. RESULTS AND DISCUSSION

4.1 Amidoximation and Characterization of Adsorbents Prepared by RIGP

The grafted AF1 adsorbent fibers were treated with 10 wt % hydroxylamine hydrochloride neutralized with KOH, for conversion of AN into AO groups. The hydroxylamine solution was prepared in different types of solvents, such as deionized water, methanol, IPA, DMSO, 50/50 (w/w) water-methanol, 50/50 (w/w) water-IPA, 20/80 (w/w) water-THF, 50/50 (w/w) water-THF, and 50/50 (w/w) water-DMSO. The amidoximation reaction with different hydroxylamine solutions was conducted at different temperatures (i.e., 60, 65, 70, 75, and 80 $^{\circ}\text{C}$) for different periods of time (i.e., 1, 3, 6, 24 h).

The Fourier Transform Infrared (FTIR) spectra of the amidoximated AF1 samples were recorded on a Perkin Elmer Frontier FTIR with a single-bounce diamond attenuated total reflectance (ATR) accessory at 2 cm^{-1} resolution and averaged over 16 scans. The FTIR spectra of AF1 amidoximated with 10 wt% hydroxylamine in different solvents at 80 $^{\circ}\text{C}$ for different time-periods are shown in Figure 2. The stretching frequency at ~ 2245 cm^{-1} is representative of the $\text{C}\equiv\text{N}$ group and thus confirms grafting of acrylonitrile onto the polyethylene. The disappearance of the nitrile stretch and appearance of $\text{C}=\text{N}$ (1650 cm^{-1}), $\text{C}-\text{N}$ (1390 cm^{-1}), $\text{N}-\text{O}$ (938 cm^{-1}), and $\text{N}-\text{H}$ (or $\text{O}-\text{H}$) (3200-3400 cm^{-1}) clearly indicates the conversion of the nitrile to amidoxime (AO). It is interesting to note that the nitrile stretches disappeared even after 1 h of amidoximation in all of the solvents except in methanol (inset, Figure 2B). The presence of nitrile stretch even after 6 h of amidoximation indicates that the reaction kinetics in methanol is slower than that in other solvents.

Astheimer et. al.⁸ and Srivastava et. al.⁹ reported formation of various functional groups, such as amidoxime, imide dioxime, hydroxamic acid and amides, upon treatment of hydroxylamine with polyacrylonitrile. Due to the very nucleophilic nature of imine nitrogen, however, the hydroxyamidine can react with adjacent nitrile groups by intermolecular cyclization leading to the formation of imide dioxime. A schematic diagram of the reaction of polyacrylonitrile with hydroxylamine is shown in Scheme 1. The ^{13}C CP/MAS spectra of AF1 adsorbent fibers are illustrated in Figure 3. The signals at 120 ppm and 176 ppm are assigned to $\text{C}\equiv\text{N}$ (i.e., acrylonitrile) and COO^- (i.e., itaconic acid), respectively,

grafted onto polyethylene. The spectra of the adsorbents amidoximated in 50:50 (w/w) H₂O-CH₃OH and DMSO at 80 °C for 1-24 h and at room temperature for 96 h are shown in Figure 3A and 3B. The signals at 157 and 149 ppm, ascribed to open-chain amidoxime and cyclic imide dioxime respectively, were observed. The signal at 120 ppm completely disappeared after amidoximation in both of the above solution at 80 °C. The incomplete disappearance of the signal at 120 ppm upon treatment in 50:50 (w/w) H₂O-CH₃OH at room temperature for 96 h indicates that the kinetics of amidoximation reaction is slower in the H₂O-CH₃OH solution as compared to DMSO. The presence of the signal at 157 ppm with a little hump at 149 ppm confirms the fact that mostly open-chain amidoxime formed after 96 h of amidoximation reaction at room temperature. The gradual increase in intensity of the 149 ppm signal and the gradual decrease of the 157 ppm signal intensity (inset Figure 3A&B) with increasing amidoximation time signifies the formation of cyclic imide dioxime by the reaction of amidoxime with adjacent cyano groups and hydroxylamine.¹⁰ It is also interesting to note that there is a small chemical shift observed in the carboxyl group (COO⁻) of itaconic acid from 176 to ~180 ppm.

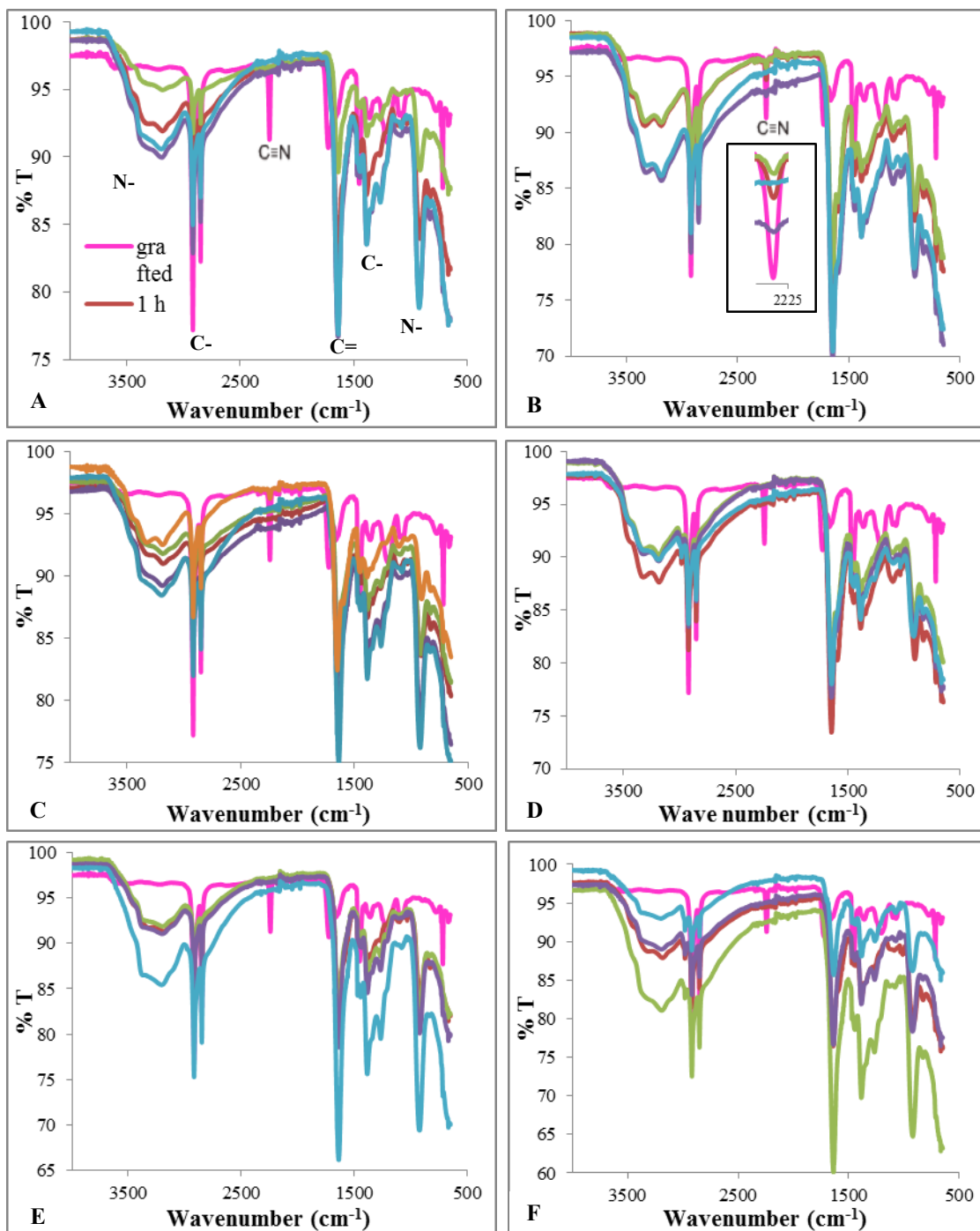
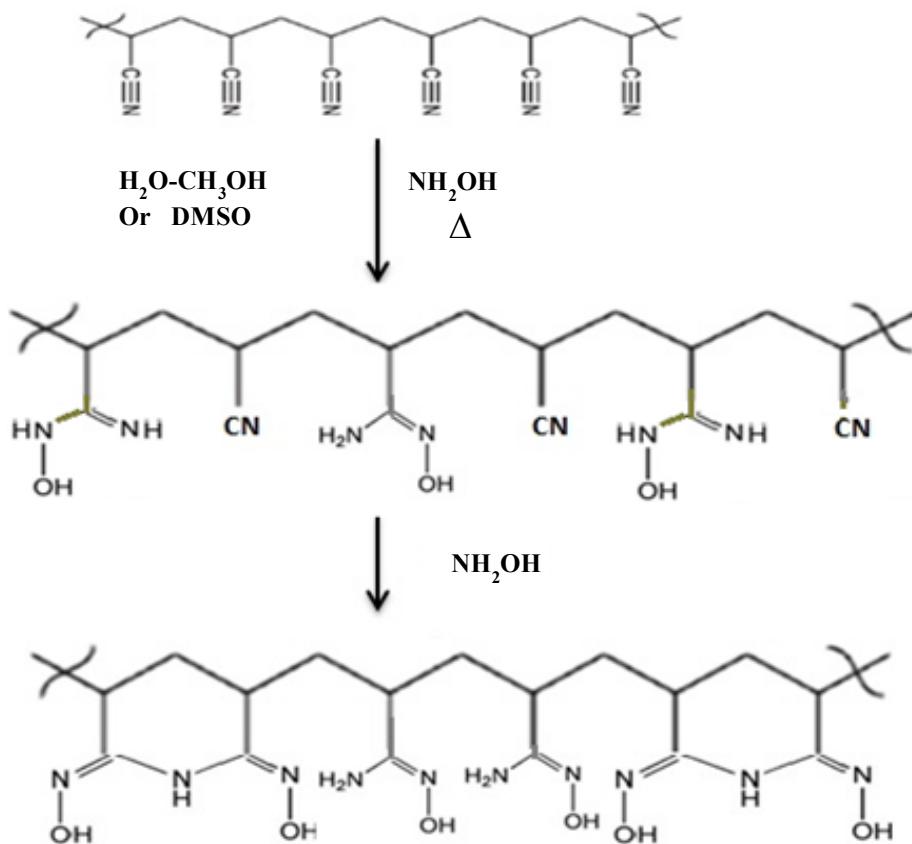


Figure 2. FTIR spectra of AF1 adsorbents amidoximated with 10 wt% hydroxylamine in (A) H₂O, (B) CH₃OH, (C) 50:50 (w/w) H₂O- CH₃OH, (D) IPA, (E) DMSO, (F) 50:50 (w/w) H₂O- DMSO, for 1, 3, 6, and 24h.



Scheme 1. Reaction mechanism of conversion of grafted polyacrylonitrile into open-chain amidoxime and cyclic imide dioxime upon treatment with hydroxylamine and heat.

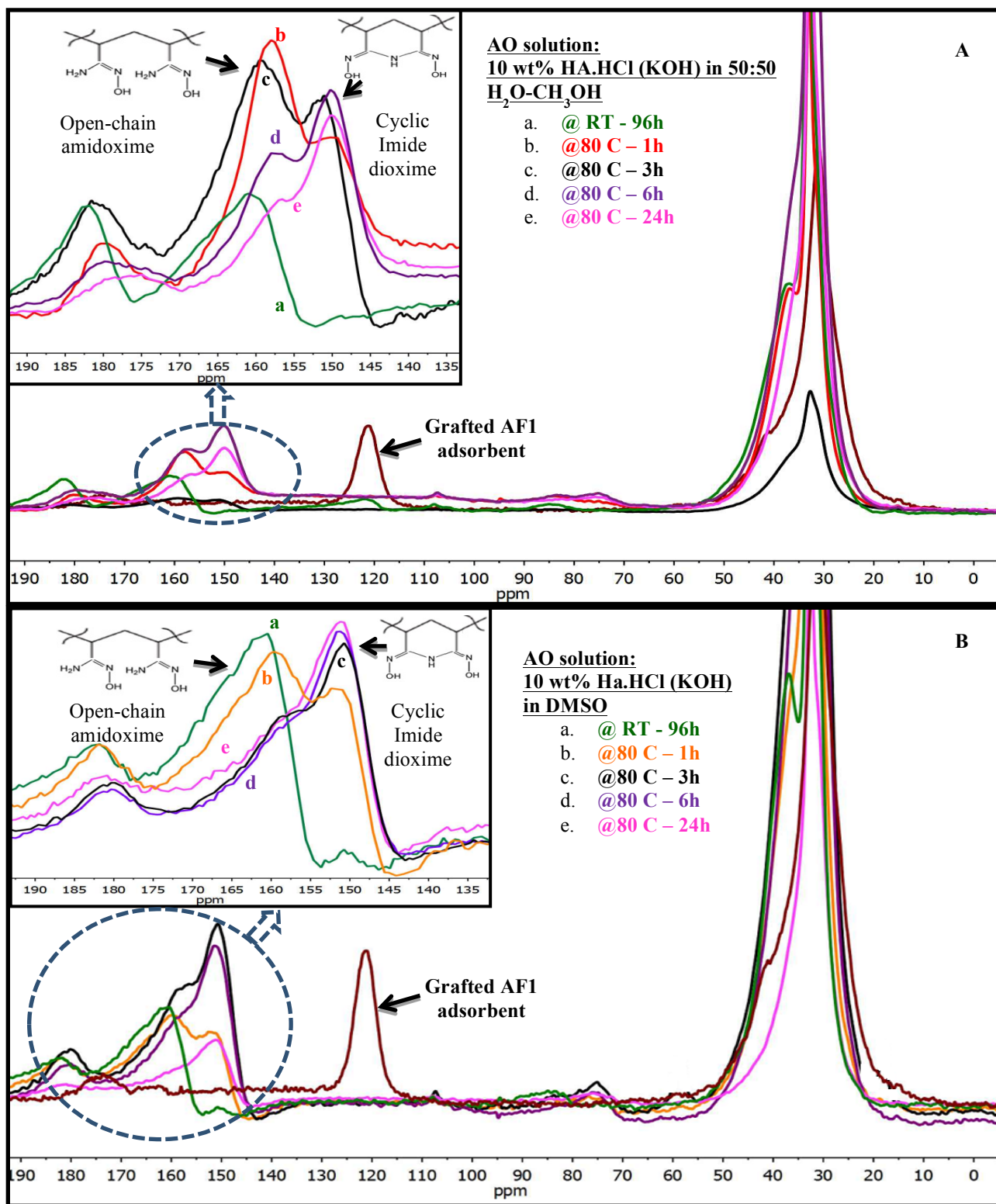


Figure 3. ¹³C CP/MAS spectra of grafted AF1, and AF1 amidoximated with 10 wt% hydroxylamine at room temperature (for 96h) and 80 °C (for 1, 3, 6, and 24 h) in (A) 50:50 (w/w) H₂O-CH₃OH, (B) DMSO.

4.1.1 Performance of adsorbents for uranium adsorption

The uranium adsorption studies of the AF1 adsorbent, amidoximated with 10 wt% hydroxylamine in different kinds of solvents for different time periods at 80 °C, after 24 h of contact with the Na-based simulated seawater solution spiked with 8 ppm uranium were carried out after conditioning with 0.44M KOH at 80 °C for 1 h. As illustrated in Figure 4A, the uranium adsorption capacity increases with increasing time of amidoximation reaction in H₂O, CH₃OH, 50:50 (w/w) H₂O-CH₃OH, IPA, 50:50 (v/v) H₂O-IPA, and 50:50 (w/w) H₂O-THF. The highest uranium adsorption was observed for the adsorbent amidoximated in DMSO and 50:50 (v/v) H₂O-DMSO for 3 h at 80 °C. The adsorbent samples were then sent to PNNL for their performance in flow-through-column tests with filtered seawater from Sequim Bay. The uranium adsorption after 21 days exposure with seawater in the flow-through-column are shown Figure 4B. The uranium adsorption capacity gradually increases with increasing amidoximation time in H₂O and 50:50 (v/v) H₂O-CH₃OH at 80 °C. The uranium uptake after 21 days was higher for the samples amidoximated in 50:50 (w/w) H₂O-CH₃OH than that in H₂O alone. On the other hand, the uranium adsorption capacity gradually decreased with increasing amidoximation time in CH₃OH. Kawakami et al.¹¹ reported that the ratio of production of imide dioxime over amidoxime was higher for the reaction of cyano group with hydroxylamine in H₂O-CH₃OH as compared to that in CH₃OH. Hence, the factors responsible for the low uranium adsorption of the AF1 sample amidoximated with CH₃OH may be (i) incomplete conversion of nitrile (Figure 2B), (ii) less amount of imide dioxime and (iii) probable chemical degradation of the adsorbent at longer reaction times. However, it is interesting to note that the AF1 samples amidoximated in DMSO resulted in the highest uranium adsorption capacity. This result was also consistent with the simulated seawater screening tests. Higher diffusivity of the DMSO solvent as compared to H₂O/CH₃OH, from the surface to the core of the grafted hollow-gear trunk PE fiber results in: (i) faster kinetics of the amidoximation reaction and (ii) larger amounts of cyclic imide dioxime throughout the adsorbent. Based on all of the above results, one can conclude that the imide dioxime was responsible either directly or indirectly for the enhanced uranium adsorption.

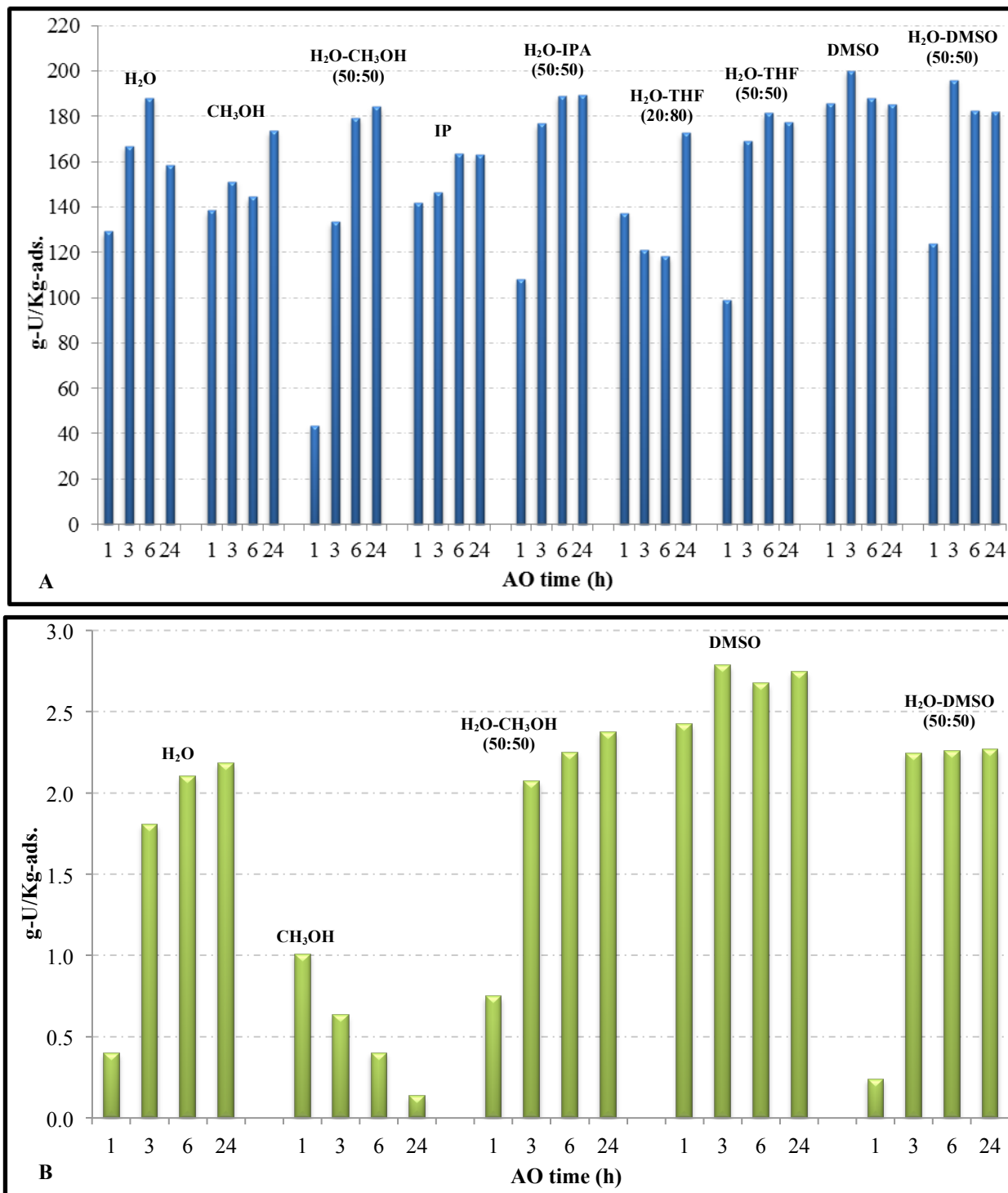


Figure 4. Uranium adsorption performance of AF1 adsorbent amidoximated with 10 wt% hydroxylamine in different solvents for different time periods at 80 °C: (A) after contacting with simulated seawater (spiked with uranium) for 24 h, (B) after 21 days exposure with seawater (Sequim Bay) in flow-through columns.

We subsequently continued our investigations for optimizing the amidoximation conditions for the AF1 adsorbents by selecting 50:50 (w/w) H₂O-CH₃OH as the standard reference solvent and DMSO as the preferred solvent. The grafted AF1 adsorbent was treated with 10% hydroxylamine in 50:50 (w/w) H₂O-CH₃OH and DMSO at different temperatures (60-80 °C) for 1, 3, 6, and 24h and at room temperature for 96 h. The uranium adsorption capacities for the amidoximated AF1 adsorbents conditioned with 0.44M KOH at 80 °C for 1 h, after 24 h of contact with the Na-based simulated seawater solution that was spiked with 8 ppm uranium, are shown in Figure 5. The uranium adsorption capacity gradually increased with an increase of reaction time in 50:50 (w/w) H₂O-CH₃OH solvent at the temperature range of 60 – 80 °C. Adsorbents amidoximated in DMSO showed higher uranium uptake but without any definite adsorption trend. On the other hand, the adsorbent amidoximated at room temperature adsorbed low amounts of uranium due to: (i) incomplete conversion of CN and (ii) the presence of only open-chain amidoxime (as shown previously in Figure 3).

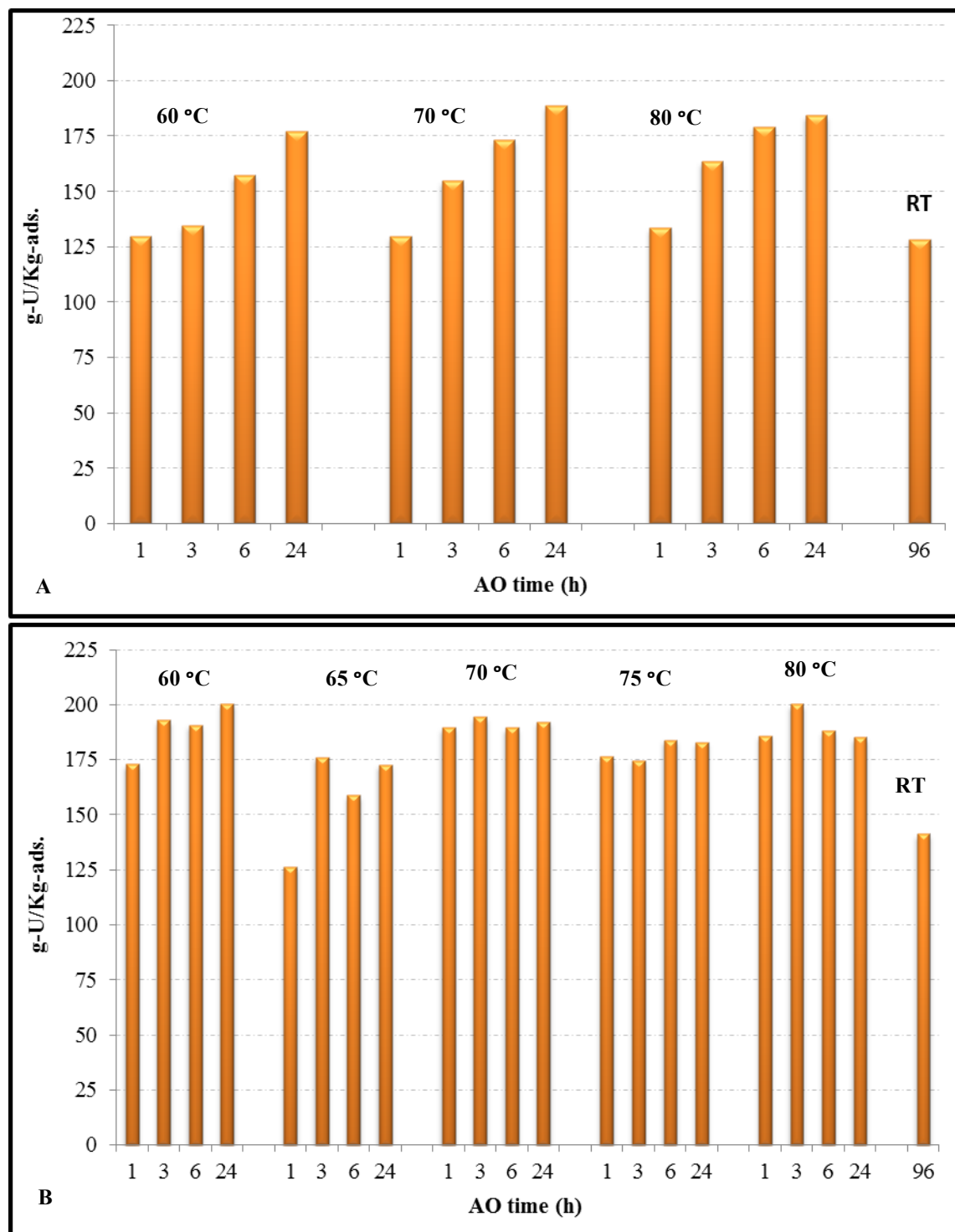


Figure 5. Uranium adsorption performance of AF1 adsorbent after contacting with simulated seawater (spiked with uranium) for 24 h. The adsorbents were amidoximated with 10 wt% hydroxylamine at different temperatures for different time periods in solvents: (A) 50:50 (w/w) H₂O-CH₃OH and (B) DMSO.

Some selected samples from the above experiments were sent to PNNL for testing in flow-through-columns. The uranium adsorption capacity results from 21 days seawater exposure in flow-through-columns are shown in Figure 6. The uranium adsorption capacities for the room-temperature amidoximated samples were relatively low. For samples amidoximated in 50:50 (w/w) H₂O-CH₃OH solvent, the uranium adsorption increases with reaction temperature and reaction time, and a temperature of 70 °C seems to be optimum (Figure 6A). For samples amidoximated in DMSO, uranium adsorption increases with reaction time and reaction temperature up to 70 °C (Figure 6B). The highest uranium adsorption capacity (~3.06 g-U/Kg--ads.) for the AF1 adsorbent after amidoximation in DMSO was achieved at 70 °C for 3 h. However, four AF1 samples amidoximated at 80 °C (for 1, 3, 6, and 24 h) and three AF1 samples amidoximated at 70 °C for 3 h (in different batches) were subsequently sent to PNNL for 56-days exposure in flow-through-column tests. The uranium adsorption capacities for AF1 samples are shown in Figure 7. As can be seen from Figure 7A, the uranium adsorption capacities for the adsorbents that were amidoximated at 80 °C gradually decreases with increasing amidoximation time, with the highest uranium adsorption of 5.04 g-U/Kg-ads. after 1 h amidoximation. On the other hand, the samples that were amidoximated at 70 °C for 3 h adsorbed the highest amount of uranium (5.06 ± 0.025 g-U/Kg-ads.) after 56 days of exposure in seawater in the flow-through-columns (Figure 7B).

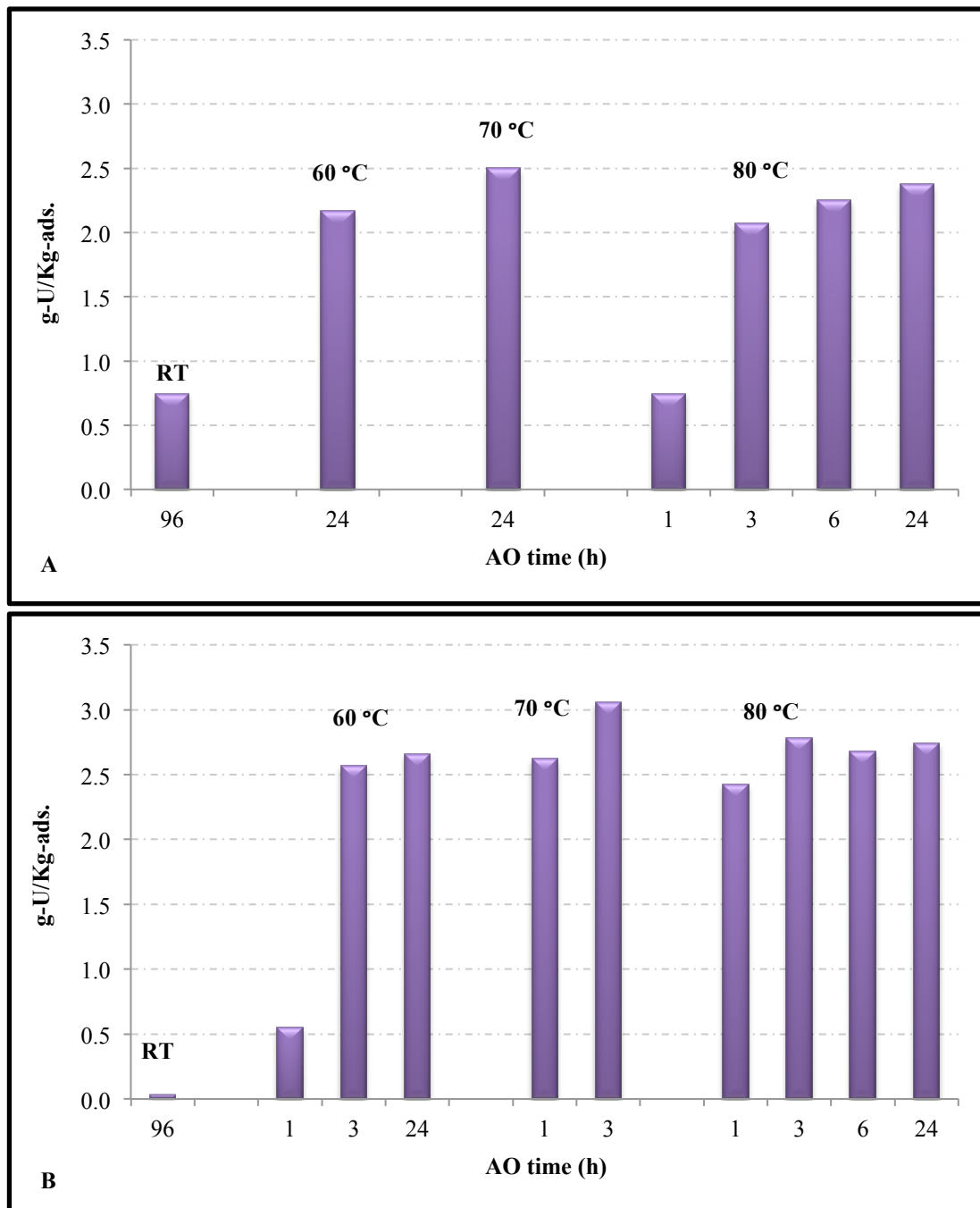


Figure 6. Uranium adsorption performance of AF1 after 21 days exposure with seawater (Sequim Bay) in flow-through columns. The adsorbents were amidoximated with 10 wt% hydroxylamine at different temperatures, for different time periods, in solvents: (A) 50:50 (w/w) H₂O-CH₃OH and (B) DMSO.

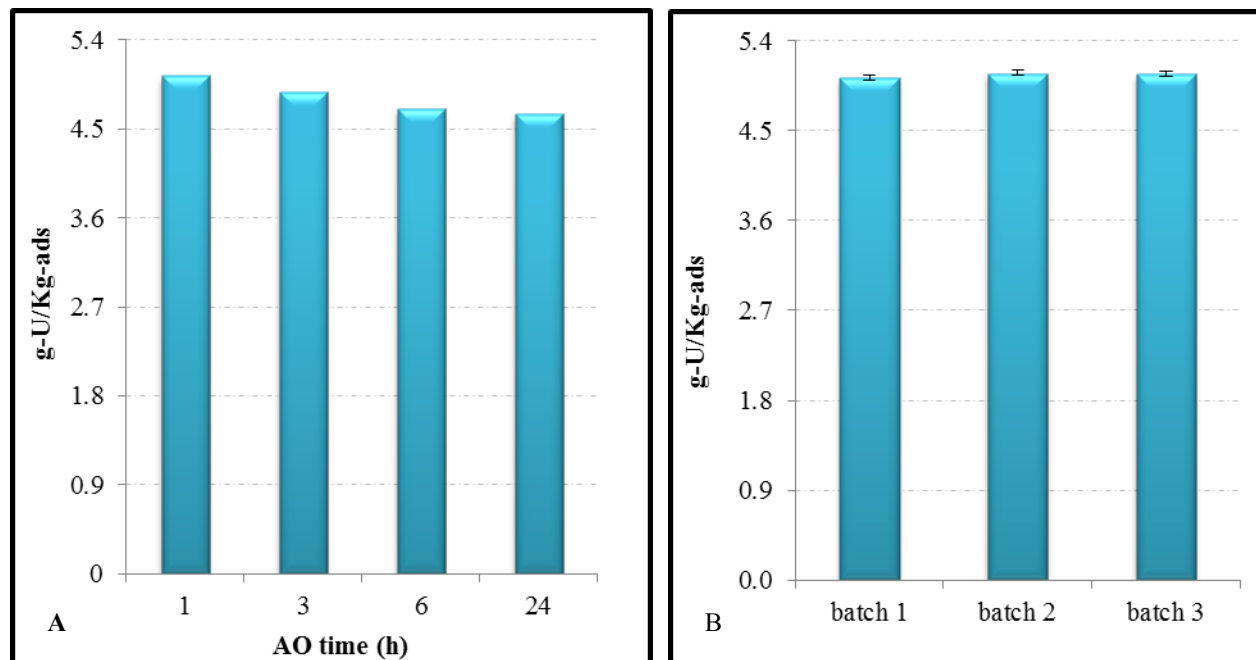


Figure 7. Uranium adsorption performance of AF1 after 56-days exposure with seawater (Sequim Bay) in flow-through columns. The adsorbents were amidoximated with 10 wt% hydroxylamine in DMSO at: (A) 80 °C for different time periods and (B) 70 °C for 3 h.

4.1.2 Kinetics of uranium adsorption

The study of adsorption kinetics of uranium by the AF1 adsorbent amidoximated in DMSO at 70 °C for 3 h was carried out in columns using filtered seawater from Sequim Bay that was passed at a flow rate of 250-300 mL/min, at 20 °C, over a period of 0-56 days. Figure 8 illustrates the relatively faster kinetics of uranium adsorption by the current adsorbent that was amidoximated in DMSO at 70 °C for 3 h compared to the conventional AF1 adsorbent, which was amidoximated in 50:50 (w/w) H₂O-CH₃OH at 80 °C for 72 h. The uranium adsorption capacity reached is 5.00 ± 0.15 g U/kg-ads after 56 days of exposure in seawater. It is interesting to note that there is a 30% enhancement in uranium adsorption capacity over the conventional AF1 adsorbent (3.86 g-U/kg-ads). Based on the data in Figure 8, a one-site ligand saturation model shows a half-saturation time of 22.9 ± 1.7 days for the AF1 adsorbent that was amidoximated in DMSO at 70 °C for 3 h, which is very similar to the conventional AF1 adsorbent (22.8 ± 1.90 days), and has a maximum (saturation) capacity of 7.05 g-U/kg adsorbent.

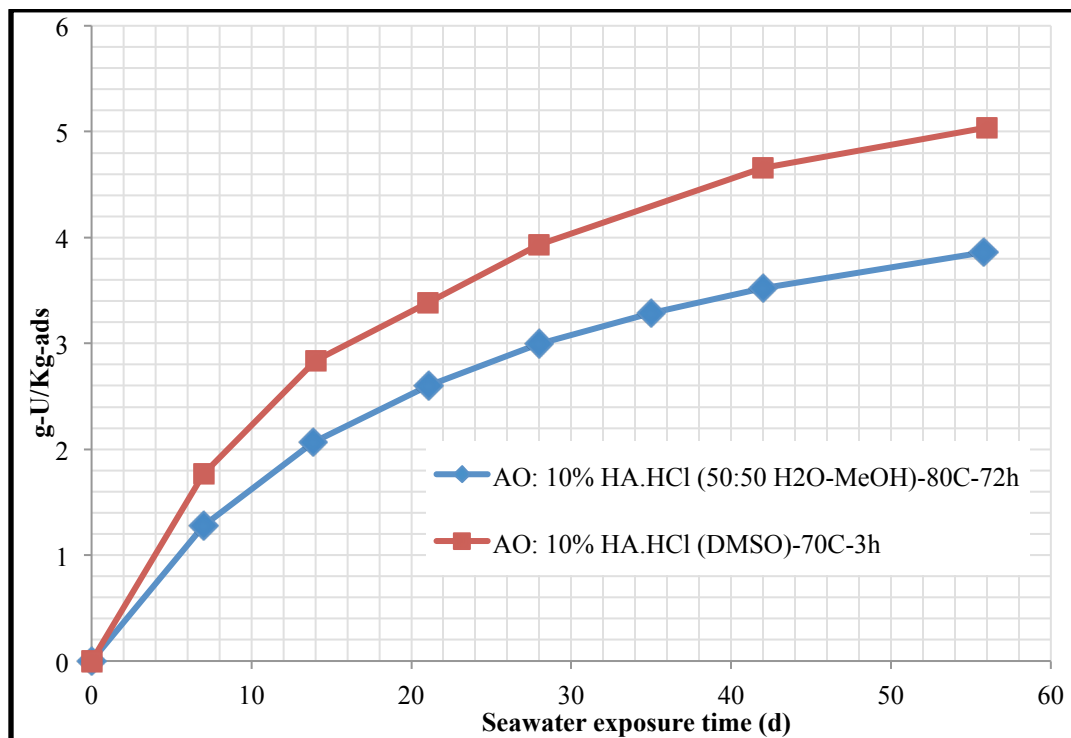


Figure 8. (A) Adsorption kinetics of uranium by the AF1 adsorbents after 56 days contact with seawater in flow-through columns.

4.1.3 Conclusions for novel adsorbents prepared by RIGP

The AF1 adsorbent comprised of acrylonitrile and itaconic acid was prepared by electron-beam induced graft polymerization onto high surface area polyethylene fibers. In searching for the optimum amidoximation reactions parameters, the conversion of grafted CN groups into AO groups was conducted in a variety of solvents such as de-ionized water, methanol, IPA, DMSO, 50/50 (w/w) water-methanol, 50/50 (w/w) water-IPA, 20/80 (w/w) water-THF, 50/50 (w/w) water-THF, and 50/50 (w/w) water-DMSO, at different temperatures. FTIR studies reveal that the conversion reaction was slow in methanol medium. The ^{13}C CP/MAS spectra of AF1 adsorbent fibers amidoximated in 50/50 (w/w) water-methanol and in DMSO clearly demonstrated the formation of open-chain amidoxime and cyclic imide dioxime. Formation of imide dioxime from amidoxime was found to occur slowly and gradually with increasing reaction time. Screening of the amidoximated samples after 24 h of contact with Na-based brine that was spiked with 8-ppm uranium showed that the uranium adsorption capacity gradually increased with amidoximation time in the water based solvents with methanol, IPA and THF, and the highest uranium adsorption capacity was observed for the samples that were amidoximated in DMSO. The performance of the adsorbents after exposure in natural seawater in the flow-through-columns was consistent with the laboratory screening results and the AF1 samples amidoximated in DMSO at 70 °C for 3 h resulted in the highest uranium adsorption capacity. We herein postulate that the higher diffusivity of DMSO as compared to $\text{H}_2\text{O}/\text{CH}_3\text{OH}$, in the grafted hollow-gear trunk PE fiber results in: (i) faster kinetics of amidoximation reaction and (ii) a larger amount of cyclic imide dioxime throughout the adsorbent. Also, imide dioxime plays an important role, directly or indirectly, to enhance the uranium adsorption from seawater. The kinetics of uranium adsorption in seawater was much faster for the sample amidoximated in DMSO at 70 °C for 3 h as compared to that in 50: 50 (w/w) $\text{H}_2\text{O}-\text{CH}_3\text{OH}$ at 80 °C for 72 h. The AF1 samples amidoximated in DMSO at 70 °C for 3 h captured 5.00 ± 0.15 g U/kg-ads. after 56 days of

exposure in seawater, which is a ~30% enhancement in uranium adsorption capacity over the conventional AF1 adsorbent that is amidoximated in water-methanol solution.

4.2 Novel Adsorbents Prepared by ATRP

4.2.1 ATRP grafting and uranium uptake in uranium-spiked brine

Synthesis of uranium adsorbent fibers were performed in three steps: 1) Simultaneous ATRP grafting of a ligand-forming monomer, AN, and a hydrophilicity-yielding monomer, HEA, from active chlorine sites on PVC-*co*-CPVC fiber; 2) AO to convert nitriles on grafted PAN to amidoximes; and 3) KOH treatment to hydrolyze HEA and unreacted AN, if any, on the grafted fibers to carboxylates, rendering hydrophilicity onto the adsorbent fibers (Figure 9). After AO, two possible structures of amidoxime-type ligands are possible: 1) acyclic amidoxime, and 2) cyclic imide dioxime converted from two adjacent amidoximes (Figure 1, final product).^{10a} It is also important to clarify that ATRP is sensitive to the presence of acids, and the solution to this problem has been to polymerize protected monomers (e.g., HEA), followed by a de-protection step (e.g., hydrolysis by KOH).¹²

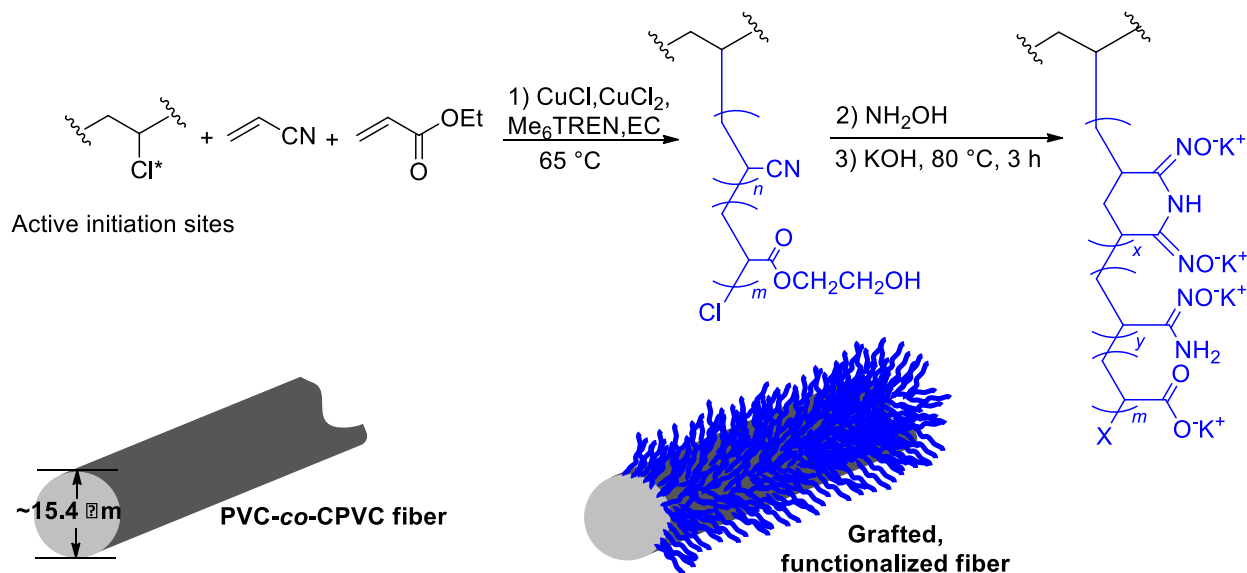


Figure 9. Synthesis steps of uranium adsorbent fibers from PVC-*co*-CPVC fibers.

The PVC-*co*-CPVC fiber used in this study is Rhovyl™'s ZCS tow fiber. It is a copolymer between PVC and CPVC, processed without any plasticizer to the round fiber form (average diameter: $15.4 \pm 2.8\ \mu\text{m}$) and without any pores that can add extra surface area to it. The measured wt % Cl from elemental analysis (EA) is 49.16%, which is lower than expected even for PVC (56.73%). The experimental value of 49.16% was used in the calculation of moles of “alkyl chlorides” (RCl). For example, for each 150-mg Rhovyl™'s fiber, $(0.150\ \text{g} \times 0.4916)/(35.453\ \text{g/mol of Cl}) = 2.08 \times 10^{-3}$ moles RCl were present. Its ¹³C CP/MAS NMR spectrum showed the expected monochloro and dichloro carbons at 58 and 97 to 91 ppm, respectively. Its methylene carbons collectively appeared at 47 ppm. Also, a broad signal ca. 200 to 100 ppm, assignable to vinyl carbons in allylic chlorides, was observed. These allylic chlorides, reportedly found in PVC,¹³ are formed as structural defects during the radical polymerization of vinyl chloride. Allylic chlorides and dichlorides were reported as actual ATRP initiation sites in PVC.¹⁴

Due to the solubility of PVC fiber in various solvents and monomers, especially at elevated temperatures, the ATRP conditions were limited to reactions in ethylene carbonate (EC) at 65 °C which allowed for reasonable polymer growth rates. Since Cu complexes formed with Me₆TREN constitute some of the

most active and reducing catalysts that were successfully employed in ATRP,¹⁵ we utilized Me₆TREN as a ligand in this study. Likewise, in our recent studies, the Cu–Me₆TREN catalyst system gave high d.g., 595–2818%, of AN and tBA from poly(vinylbenzyl chloride) initiation sites.¹⁶

In order to identify the optimal amount of catalyst, the ATRP grafting of AN under various amounts of CuCl, from 0.75 [CuCl]/993 [AN] to 2.0 [CuCl]/993 [AN], was performed along with uranium uptake tests on corresponding amidoximated fibers (Table 1). The d.g. of the resulting fibers did not drastically differ with varying concentrations of catalyst. However, due to the higher d.g. and enhanced U uptake performance (i.e., higher U adsorption capacity and distribution coefficient, K_d), of fibers obtained with a [AN]/[RCl]/[CuCl]/[Me₆TREN]/[CuCl₂] ratio of 993:5.4:1.0:1.2:0.050 (Table 1, no. 1.2), this reactant-to-catalyst ratio was used as a guideline for the rest of this study. It is also worth mentioning that homopolymerization was not observed under the reaction conditions studied (i.e., precipitate was not formed when the reaction mixture was added into 50% aqueous-methanol solution).

Table 1 ATRP of AN and uranium uptake in 750-mL U-spiked brine

[AN]/[RCl]/[CuCl]/ [Me ₆ TREN]/[CuCl ₂] ^a	d.g., %	U adsorption capacity, g/kg
993:5.4:0.75:0.90:0.038	408	94.1
993:5.4:1.0:1.2:0.050	437	116.5
993:5.4:1.5:1.8:0.075	362	63.5
993:5.4:2.0:2.4:0.10	356	106.6

^a Constant ratio between CuCl, Me₆TREN, and CuCl₂, in 50 vol % EC, 65 °C, 24 h.

With the catalyst concentration held constant, the [AN]/[HEA] feed ratio was varied in simultaneous copolymerization (Table 2). The elemental analysis (EA) of the N and O contents of the grafted fibers permitted the calculation of the [PAN]/[PHEA] ratios (fourth column). As expected, the [PAN]/[PHEA] ratios of the grafted fibers decreased with decreasing [AN]/[HEA] feed ratio. However, the [PAN]/[PHEA] ratios were slightly higher than the corresponding [AN]/[HEA] feed ratios, indicating a more efficient grafting of PAN than PHEA. Overall, high d.g. values were obtained, especially at lower [AN]/[HEA] feed ratios. These d.g. values were much higher than the values normally obtained from RIGP grafting of functional monomers from backbone fibers.¹⁷

Table 2 Simultaneous copolymerization of AN and HEA

No.	[AN]/[HEA] ^a	[AN]/[HEA], ratio of mol % (feed)	[PAN]/[PHEA], ratio of mol % (EA)	dg, %
A1	500:125	80.0:20.0		306
A2	500:250	66.7:33.3	71.4:28.6	1041
A3	500:375	57.1:42.9	63.7:36.3 to 67.1:32.9 ^b	1710 to 1823 ^b
A4	500:500	50.0:50.0	56.5:43.5	2900

^a [AN]/[HEA]/[RCl]/[CuCl]/[Me₆TREN]/[CuCl₂] = the above monomer ratios:5.4:1.0:1.2:0.05, in 50 vol % EC, 65 °C, 24 h.

^b [PAN]:[PHEA] ratios from four repeated experiments.

At first, a standard amidoximation procedure (i.e., 80 °C for 2 days then 1 day) was used for the preparation of adsorbent fibers and KOH treatment conditions were varied. Figure 10 shows the results from screening tests in a uranyl brine consisting of seawater-relevant concentrations of sodium, chloride, and bicarbonate (pH ~ 8) spiked with 6 ppm U. Comparing the different formulas of fiber grafting, A1 through A4, fiber A3 showed the highest U adsorption capacities. This demonstrated the importance of obtaining an optimized ligand:hydrophilic group ratio (i.e., [PAN]:[PHEA] ratio).¹⁸ When [PAN]:[PHEA]

ratio was not optimized, the U adsorption capacity decreased, even in fibers with high d.g. values. Comparing the various conditions of KOH treatment, longer KOH treatment time, up to 3.5 h, increased the U adsorption capacity of adsorbent fibers (Figure 10). In a separate experiment, longer KOH treatment time resulted in lower uranium uptake. Uranium adsorption capacities of 146.8 and 110.9 g/kg were obtained from 3-h and 4-h KOH, respectively, on fiber A3 amidoximated at 25 °C for 5 days (graph not shown). Fiber A3 and 3.5-h KOH treatment were therefore used for most of the study reported here.

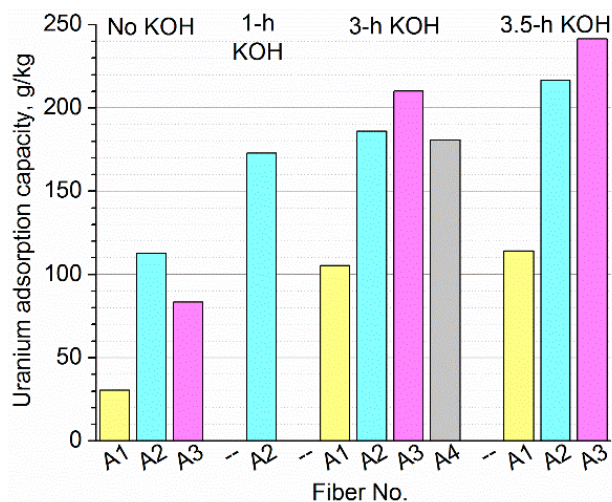


Figure 10. Uranium uptake in 750-mL U-spiked brine (Different grafted fibers, AO'd at 80 °C for 2 days followed by 1 day, varied KOH treatment at 80 °C).

A blank experiment was also conducted on PVC-*co*-CPVC backbone fiber (AO: 2 d then 1 d at 80 °C, KOH: 3 h at 80 °C) and AO'd and grafted PHEA fiber (AO: 2 d then 1 d at 80 °C, KOH: 3.5 h at 80 °C), resulting in negligible U adsorption capacities of 0.49 and 0.20 g U/kg, respectively. This indicates that the high U adsorption capacities in fibers A1 through A4 were originated from the grafted PAN.

4.2.2 Characterization of adsorbent fibers prepared by ATRP

Adsorbent fibers were characterized by solid-state ¹³C NMR (Figure 11). On the grafted fiber A3 (trace (a) in Figure 11), signals from -COOR in PHEA (174 ppm), -CN in PAN (119 ppm), and $\text{-OCH}_2\text{CH}_3$ carbons in PHEA (67 and 60 ppm) were observed as expected. After AO at 80 °C (trace (b) in Figure 11), a new signal (150 ppm) assigned to cyclic imide dioxime appeared. This signal was broad and plausibly accompanied by an obscure shoulder (157 ppm) assigned to acyclic amidoxime,^{10b, 17} indicating an incomplete cyclization even after long amidoximation time. In agreement with literature reports, the cyclic imide dioxime is expected to be the major product obtained from AO reactions in aqueous solutions at elevated temperatures.^{10, 17, 19} The formation of cyclic imide dioxime also indicates that simultaneous grafting of AN and HEA did not yield completely random copolymers. Around 119 ppm, the majority of -CN signal was no longer observed. In the carbonyl region, a new signal from -COO^- (182 ppm) appeared in a relatively equal intensity to the signal from -COOR (175 ppm) in PHEA, indicating that partial hydrolysis of PHEA occurred during AO. This is in agreement with the weight loss of the fibers observed during AO.

After a 3.5-h KOH treatment at 80 °C (c), the signal from -COO^- (184 ppm) became prominent, while the signal from -COOR (174 ppm) remained at much lower intensity, indicating that a significant degree of hydrolysis of PHEA occurred. Along with the cyclic imide dioxime signal (150 ppm), the small shoulder from the acyclic amidoxime (158 ppm) became more pronounced, indicating that some decomposition of cyclic imide dioxime occurred during the KOH treatment.

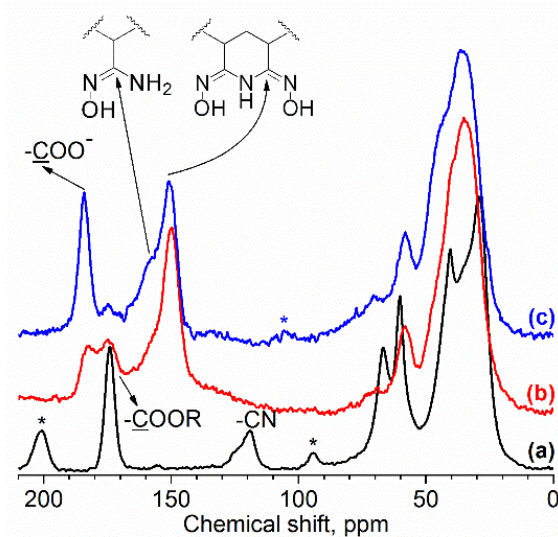


Figure 11. 100 MHz ^{13}C CP/MAS NMR spectra of fibers as (a) grafted (fiber A3), (b) amidoximated (2 d then 1 d at 80 °C), and (c) KOH-treated (3.5 h at 80 °C). Asterisk (*) denotes spinning sideband (spinning speed = 8.0 kHz).

4.2.3 Uranium uptake of ATRP fiber adsorbents in seawater

Adsorbent fibers showing uranium adsorption capacities of > 150 g/kg in the uranium-spiked brine were selected for continuous-flow column experiments in seawater at the Marine Sciences Laboratory of PNNL at Sequim Bay, WA (Table 3). With a standard amidoximation procedure (80 °C for 2 days then 1 day) and 3.5-h KOH treatment, fiber A3, which showed the highest U adsorption capacity in brine (Figure 10), also showed the highest adsorption capacity, 5.61 and 6.11 g/kg (data from two batches of fibers), in environmental seawater after a 42-day exposure. Fibers A2 and A4 showed lower adsorption capacities as also observed in the brine tests. Among the fibers A3 amidoximated at two different temperatures, AO at 25 °C yielded lower uranium adsorption capacity than that from AO at 80 °C.

Table 3 Uranium uptake in seawater at Sequim bay, WA

No.	AO	KOH treatment	42-d (PNNL) ^a	
			g/kg	V/U (wt ratio)
A2	80 °C 2 d then 1 d	80 °C 3.5 h	2.98, 3.46	2.7, 3.5
A3	80 °C 2 d then 1 d	80 °C 3.5 h	5.61, 6.11	2.6, 2.0
A4	80 °C 2 d then 1 d	80 °C 3.5 h	3.52, 3.74	2.3, 2.3
A3	25 °C 5 d	80 °C 3.5 h	0.57, 2.76	3.0, 1.7

^a Normalized to a salinity of 35 psu. Some experiments were repeated to check the reproducibility.

The kinetics of the metal uptake was studied on two batches of the fiber A3 in order to confirm the reproducibility of the fiber's performance (Figure 12 and Table 4). The adsorbent fibers were prepared by repeating the same experiments, from ATRP through KOH treatment and exposure time with natural seawater. The results showed unprecedentedly high uranium adsorption capacities, with good reproducibility, of the fiber A3.

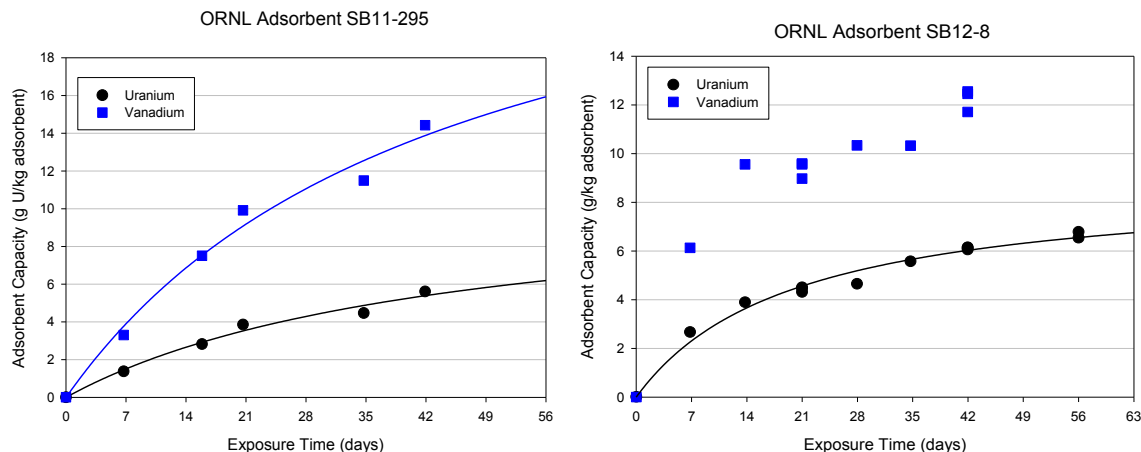


Figure 12. Kinetic plots of uranium and vanadium uptake of two batches of fiber A3 in Sequim Bay, WA, with one-site ligand saturation modeling (salinity normalized to 35 psu).

Table 4. Uranium adsorption capacity from one-site ligand saturation modeling

Batch	56-d adsorption capacity, g/kg	adsorption capacity, g/kg	half- saturation time, days	r^2
1	6.18 ± 1.34	11.1 ± 2.4	44.6 ± 16.4	0.983
2	6.56 ± 0.33	8.90 ± 0.45	20.0 ± 2.65	0.984

4.2.4 Economic analysis of ATRP-based fiber adsorbents

The cost of recovering uranium using this adsorbent is estimated by applying discounted cash flow techniques to the lifecycle of a unit mass of adsorbent. The cost assessment methodology used here has been applied to multiple adsorbent technologies.^{20,21,22,23,24,25} The methodology is presented in detail elsewhere²⁰ and unless explicitly noted the input cost data used here are the same as those provided in that publication. Costs are given in year 2015 dollars.²⁶ The analysis assumes that the slightly positively buoyant adsorbent braids are moored to the seabed and deployed in the ocean in a kelp-field like structure,^{27,28} and the deployment costs associated with this scheme were analyzed in a later article.²⁴ Upon completion of their soaking campaign the braids are winched up so the uranium may be eluted off before they are re-deployed. This novel adsorbent is assumed to offer structural integrity similar to that of polyethylene fibers analyzed in past work, so costs associated with each deployment and mooring event are unchanged from the previous determination.²⁴ The number of times the adsorbent is reused is allowed to vary, as its optimal value is dependent upon the rate of degradation caused by elution as well as exposure to seawater.

A cost estimate is first produced for the demonstrated reference procedure described in previous sections and opportunities for reducing cost further are subsequently explored. The chemical consumption rates for the ATRP grafting procedure are derived from the reported degree of grafting and elemental analyses which determined the mass ratio of acrylonitrile to co-monomer grafted on the fiber. It is assumed that all solvents and catalysts can be re-used with a recovery rate of 90% and all other chemicals are consumed with negligible losses. Major cost drivers in the adsorbent production process are then identified and a cost estimate produced for a second case where potential cost benefits of advantageous modifications to the process are explored.

New data that is unique to this work includes chemical and raw material costs specific to this adsorbent type. As in previous methodologies most of these costs are determined by obtaining vendor quotes for bulk orders using the Chinese e-commerce company Alibaba, which specializes in connecting large scale producers with commercial customers. For some chemical commodities, however, commercial availability and the size of the world industry were found to be so limited that economies of scale must be taken into account to reflect the change in chemical cost that would result from the significant increase in total demand should this adsorbent be produced on an industrial scale,²⁹ as was the case for the Me₆TREN. An exception is the cost of the Rhovyl™ fibers themselves, which was obtained directly from Rhovyl representatives.

Table 5 displays cost data for chemical inputs unique to this adsorbent; all others can be found in a previous publication.²⁰ Figure 13 shows the mass balance for this process normalized to a unit mass of Rhovyl™ fiber. The values in the green bubbles indicate mass consumed while the orange rectangles represent catalysts and solvents so the masses indicated must be present, although 90% of this is assumed to be recovered.

Table 5 Price for bulk orders of chemical inputs

Chemical	Cost (\$/tonne)
Rhovyl™ Fiber	10,100
2-hydroxyethyl Acrylate	1,700
Ethylene Carbonate	2,200
Copper (II) Chloride	4,700
Me ₆ TREN	870,000
Copper (I) Chloride	8,200
PMDETA	4,500
CPVC Resin	1,500

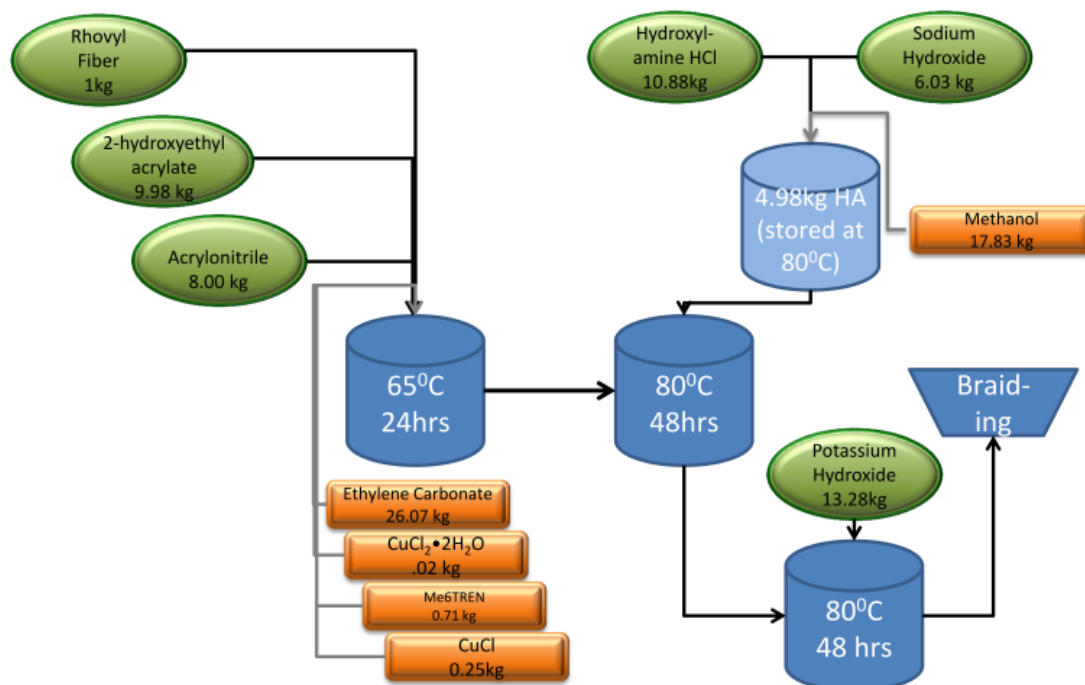


Figure 13 Process flow diagram for adsorbent production via ATRP.

There are significant uncertainties surrounding the performance of the adsorbent in the ocean environment. Notably, experimentation in seawater has shown that a loss in uptake of up to 30% may be expected due to oceanic biofouling. This data comes from experiments conducted with an amidoxime based High Density Polyethylene (HDPE) adsorbent.³⁰ There is not yet data for the effects of biofouling on the SB12-8 adsorbents, but since the fiber morphologies are broadly similar, the 0-30% capacity loss specified in Table 6 is expected to be appropriate. The 30% upper-bound set on the effects of biofouling is likely higher than what will actually be seen in reality; light and temperature conditions where the braids will be deployed, 100 meters beneath the surface, are potentially less conducive to bioactivity than the laboratory conditions in the referenced experiments. Differences in fiber topography as compared to HDPE may play a role in the degree of marine-organism colonization, which has not yet been quantified. Similarly, the data for degradation upon adsorbent re-use comes from the HDPE adsorbents but is expected to be applicable. The most severe degradation case is derived from recent experiments at ORNL and PNNL³¹ showing that loss in uptake was a function of length of campaign and number of re-uses. Longer soaking campaigns were seen to exacerbate capacity loss. The lower limit of a consistent 5% loss in uptake per re-use has been seen on amidoxime based adsorbents created in Japan.³² Given these uncertainties, uranium production cost must be presented as a range. The parameters giving rise to this range are displayed in Table 6.

Table 6 Base case parameters

Parameter	Value
Adsorbent Material	SB12-8
Degree of Grafting (%)	1900
Alkaline Solution	KOH
Length of Campaign (days)	Optimized for each scenario
Number of Uses	Optimized for each scenario
Temperature (200C)	20
Biofouling (% loss in uptake)	0-30
Degradation (% loss per re-use)	5-Worse case

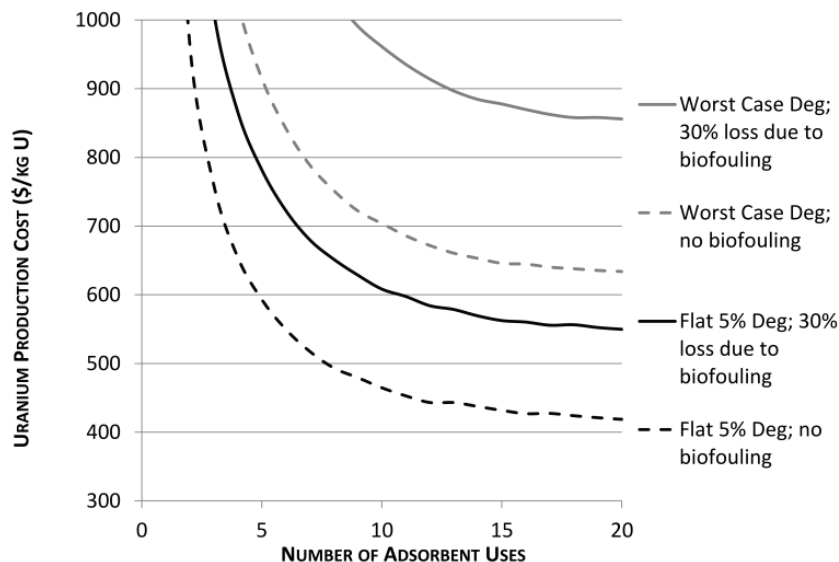


Figure 14 Uranium production cost for case 1 as a function of number of adsorbent uses.

Given the cost data in Table 6 and performance parameters in Table 6, a uranium production cost ranging from \$420-860/kg U is found (Fig. 14). Each line represents a degradation/biofouling scenario, and in every case the days of campaign and number of adsorbent uses are optimized to achieve the lowest uranium production cost for the given degradation/biofouling level. The optimal number of uses is constrained not to exceed 20 due to a lack of experimental data at this high number of uses. In the case of a constant 5% adsorbent degradation rate, the optimal soaking campaign is around 50 days, while the worst case degradation optimizes closer to 10 days of exposure. The cost range achieved by this adsorbent can be compared against the amidoxime-based HDPE adsorbents, which yielded a uranium production cost of \$440-960/kg U for analogous reference ranges.³³ The cost decrease, roughly 10%, is predominantly a result of the improvement in adsorbent capacity, as this has been previously identified as one of the most significant cost drivers³⁴.

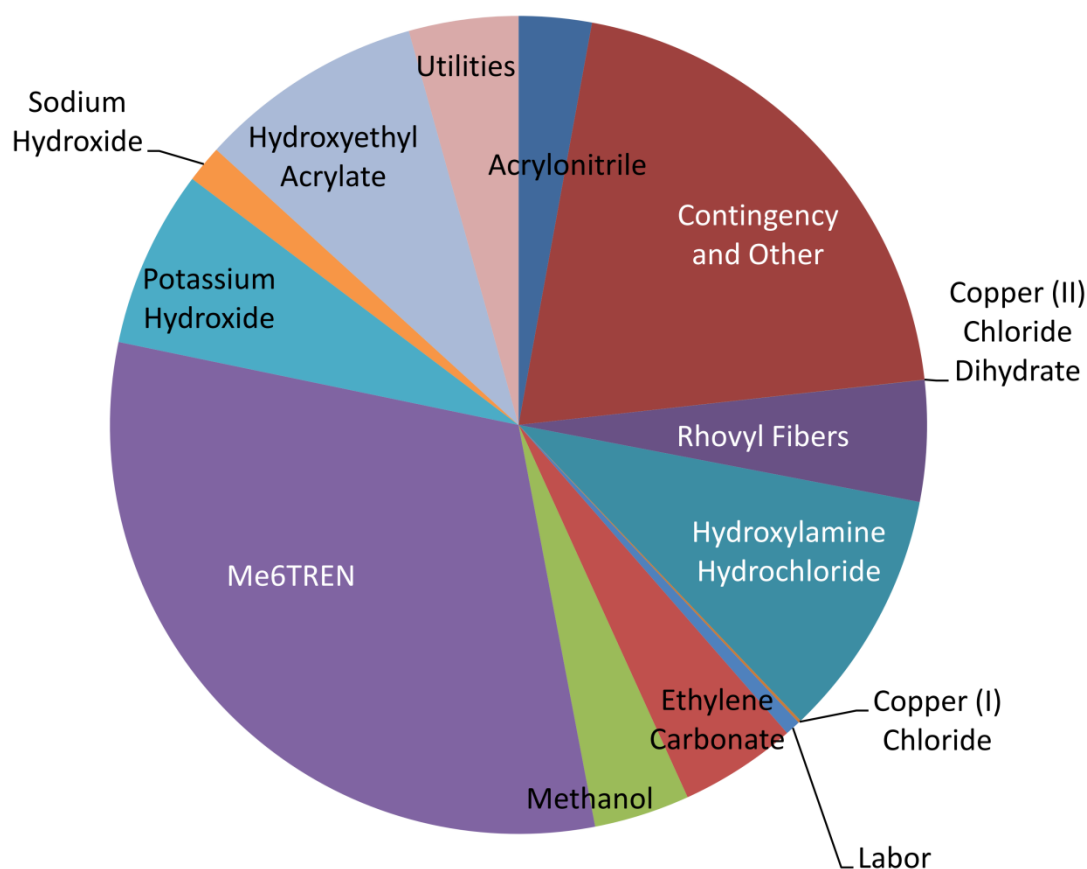


Figure 15 Breakdown of adsorbent production operating and maintenance cost.

A breakdown of the adsorbent production cost exclusive of capital expenses is shown in Figure 15 and serves to highlight areas where savings may be achieved. It is clear that the Me₆TREN makes up a large portion of the adsorbent production cost. While the consumption rate of Me₆TREN is not large, the cost is extremely high, even taking into account economies of scale, in part because this chemical is not commonly used on an industrial scale. Another area for potential cost savings is the Rhovyl fibers. This premanufactured CPVC substrate is around seven times more expensive per unit mass than HDPE resin, although the HDPE must be formed into fibers. Due to the very high degree of grafting, the adsorbent contains little CPVC fiber by mass, so this low consumption rate results in the comparatively small contribution to final adsorbent production cost. A cheaper adsorbent backbone allows for lower degrees of grafting, may turn out to be favorable, without a price increase.

Next, a second cost range is developed. This estimate uses the same range of parameters displayed in Table 6, but addresses the potential cost benefits of alternatives to the aforementioned cost drivers. Initial experiments have used PVC-co-CPVC fibers purchased from Rhovyl™. In an effort to reduce cost, the current cost estimate presumes that fibers of similar quality can be made in house for a reduced cost by extruding CPVC resins, analogous to previously-studied cases where raw high density polyethylene was melt-spun into fibers. The same methodology used in previous cost estimates^{21,20} was used to determine the capital and labor cost associated with the melting, single-screw extrusion, and spinning of polymer resins. According to Rhovyl™ product specifications the fibers consist of 70% PVC (57 wt % Cl) and 30% super-chlorinate PVC made with no plasticizer (personal communication); given that pure CPVC is 85% Cl by weight, any CPVC with ~65 wt% Cl and free of plasticizer should be sufficient for this adsorbent.

Additionally, the expensive Me₆TREN catalyst may be replaceable by less costly pentamethyldiethylenetriamine (PMDETA). The cost of PMDETA was determined using the same methodology as previously mentioned chemicals to be \$4,500/tonne, significantly cheaper than Me₆TREN. Although the use of PMDETA as a substitute has not yet been proven experimentally, it is being considered on the basis of the cost savings identified here.

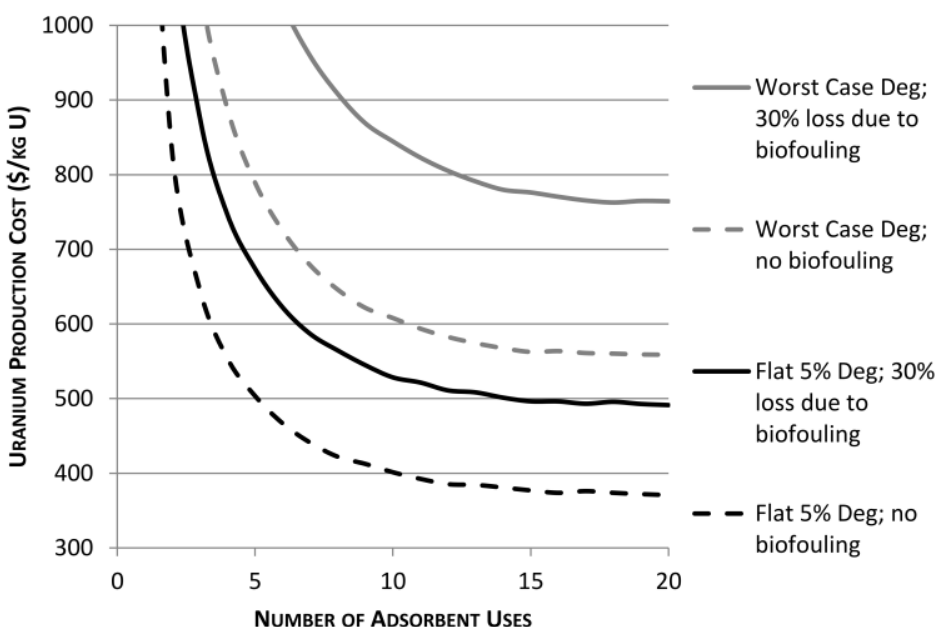


Figure 16 Uranium production cost as a function of number of adsorbent uses for case 2.

Assuming these updates can be carried out without adverse effects on uptake, the resulting cost range decreases to \$370-760/kg U, a cost savings of ca. 12%. Figure 16 shows the uranium production cost for this second case as a function of adsorbent uses. As before, each scenario is optimized to the ideal campaign length. The uranium production cost breakdown by activity area for an arbitrarily chosen case intermediate to the degradation and biofouling extremes is displayed in Figure 17, where case 1 represents the original, experimentally demonstrated procedures, while case 2 implements the PMDETA and substrate changes. In both cases, degradation is modeled as the worst case scenario while the effects of biofouling are neglected. Significant reduction in the adsorbent production operating expenses can be seen in case 2 due to the use of PMDETA and custom extruded fibers. This is partly offset by an increase

in the adsorbent production capital cost resulting from the equipment to conduct the melt-spinning of the polymer resins.

These novel adsorbents offer uranium production costs that are very competitive with the best available alternatives, especially if the proposed changes can be realized. Moving forward to reduce the cost, it will be experimentally proven that PMDETA can in fact replace Me₆TREN. In order to reduce the uncertainty and tighten the cost interval, better characterization of the degradation rate upon adsorbent reuse, as well as the loss in uptake due to marine biofouling, are needed.

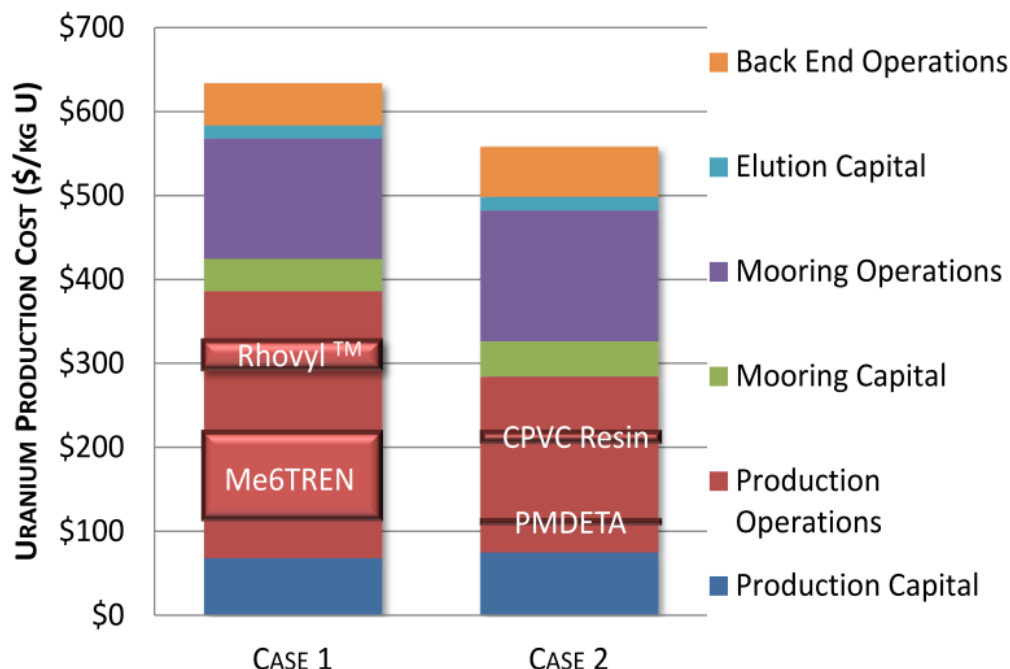


Figure 17 Comparison of cost breakdown for cases 1 and 2.

4.2.5 Conclusions for novel adsorbents prepared by ATRP

Novel fiber adsorbents prepared by ATRP of HEA, HEMA, and AN. The composition of grafted chain was optimized, resulting in a significant increase on the uranium adsorption capacity. The optimized ATRP adsorbent achieved 6.56 ± 0.33 g U/kg-ads., after 56 days of seawater exposure, which is the highest ever reported. With this capacity, an estimated uranium production cost ranges from \$420-860/kg or \$370-760/kg, which is so far the best cost efficiency. This study successfully exceeded the goal of this milestone to develop new fiber materials with sorption capacity at 5.0 g-U/kg adsorbent under marine testing conditions. Further optimization, investigation of other new materials, as well as deepening our understanding will result in the development of novel adsorbents that have even higher uranium adsorption capacities, increased selectivity, and faster kinetics.

Acknowledgment

This work was sponsored by the Office of Nuclear Energy of the U.S. Department of Energy.

References

1. Report of the Working Party on Extraction of Uranium from Sea-Water. United Kingdom Atomic Energy Authority. **1976**.
2. (a) Saito, K.; Uezu, K.; Hori, T.; Furusaki, S.; Sugo, T.; Okamoto, J., Recovery of uranium from seawater using amidoxime hollow fibers. *AIChE J.* **1988**, *34* (3), 411–416; (b) Yue, Y. F.; Mayes, R. T.; Kim, J.; Fulvio, P. F.; Sun, X. G.; Tsouris, C.; Chen, J. H.; Brown, S.; Dai, S., Seawater uranium sorbents: Preparation from a mesoporous copolymer initiator by atom-transfer radical polymerization. *Angewandte Chemie-International Edition* **2013**, *52* (50), 13458–13462.
3. Kim, J.; Tsouris, C.; Oyola, Y.; Janke, C. J.; Mayes, R. T.; Dai, S.; Gill, G.; Kuo, L.-J.; Wood, J.; Choe, K.-Y.; Schneider, E.; Lindner, H., Uptake of Uranium from Seawater by Amidoxime-Based Polymeric Adsorbent: Field Experiments, Modeling, and Updated Economic Assessment. *Industrial & Engineering Chemistry Research* **2014**, *53* (14), 6076–6083.
4. (a) Das, S.; Oyola, Y.; Mayes, R. T.; Janke, C. J.; Kuo, L. J.; Gill, G.; Wood, J. R.; Dai, S., Extracting Uranium from Seawater: Promising AI Series Adsorbents. *Industrial & Engineering Chemistry Research* **2015**; (b) Das, S.; Oyola, Y.; Mayes, R. T.; Janke, C. J.; Kuo, L. J.; Gill, G.; Wood, J. R.; Dai, S., Extracting Uranium from Seawater: Promising AF Series Adsorbents. *Industrial & Engineering Chemistry Research* **2015**; (c) Kim, J.; Tsouris, C.; Oyola, Y.; Janke, C. J.; Mayes, R. T.; Dai, S.; Gill, G.; Kuo, L. J.; Wood, J.; Choe, K. Y.; Schneider, E.; Lindner, H., Uptake of uranium from seawater by amidoxime-based polymeric adsorbent: Field experiments, modeling, and updated economic assessment. *Industrial & Engineering Chemistry Research* **2014**, *53* (14), 6076–6083.
5. Seko, N.; Katakai, A.; Hasegawa, S.; Tamada, M.; Kasai, N.; Takeda, H.; Sugo, T.; Saito, K., Aquaculture of uranium in seawater by a fabric-adsorbent submerged system. *Nuclear Technology* **2003**, *144* (2), 274–278.
6. Saito, T.; Brown, S.; Chatterjee, S.; Kim, J.; Tsouris, C.; Mayes, R. T.; Kuo, L. J.; Gill, G.; Oyola, Y.; Janke, C. J.; Dai, S., Uranium recovery from seawater: development of fiber adsorbents prepared via atom-transfer radical polymerization. *Journal of Materials Chemistry A* **2014**, *2* (35), 14674–14681.
7. (a) Brown, S.; Chatterjee, S.; Li, M.; Yue, Y.; Tsouris, C.; Janke, C. J.; Saito, T.; Dai, S., Uranium Adsorbent Fibers Prepared by Atom-Transfer Radical Polymerization from Chlorinated Polypropylene and Polyethylene Trunk Fibers. *Industrial & Engineering Chemistry Research* **2015**; (b) Brown, S.; Yue, Y.; Kuo, L.-J.; Mehio, N.; Li, M.; Gill, G. A.; Tsouris, C.; Mayes, R. T.; Saito, T.; Dai, S., Uranium adsorbent fibers prepared by ATRP from PVC-co-CPVC fiber. *Industrial & Engineering Chemistry Research* **2016**.
8. Astheimer, L.; Schenk, H. J.; Witte, E. G.; Schwochau, K., Development of sorbers for the recovery of uranium from seawater. 2. The accumulation of uranium from seawater by resins containing amidoxime and imidoxime functional groups. *Separation Science and Technology* **1983**, *18* (4), 307–339.
9. Srivastava, R. M.; Brinn, I. M.; MachucaHerrera, J. O.; Faria, H. B.; Carpenter, G. B.; Andrade, D.; Venkatesh, C. G.; deMorais, L. P. F., Benzamidoximes: Structural, conformational and spectroscopic studies .1. *Journal of Molecular Structure* **1997**, *406* (1-2), 159–167.
10. (a) Kang, S. O.; Vukovic, S.; Custelcean, R.; Hay, B. P., Cyclic imide dioximes: Formation and hydrolytic stability. *Industrial & Engineering Chemistry Research* **2012**, *51* (19), 6619–6624; (b) Kobuke, Y.; Tanaka, H.; Ogoshi, H., Imidedioxime as a significant component in so-called amidoxime resin for uranyl adsorption from seawater. *Polymer Journal* **1990**, *22* (2), 179–182.
11. Kawakami, T.; Akiyama, E.; Hori, K.; Nagase, Y.; Sugo, T., Structural changes of compounds containing cyano groups by hydroxylamine treatment. *Transactions of the Materials Research Society of Japan* **2002**, *27* (4), 783–786.
12. Davis, K. A.; Matyjaszewski, K., Atom transfer radical polymerization of *tert*-butyl acrylate and preparation of block copolymers. *Macromolecules* **2000**, *33* (11), 4039–4047.

13. Benedikt, G. M.; Goodall, B. L.; Rhodes, L. F.; Kemball, A. C., NMR-spectroscopy of poly(vinyl chloride) defects. 2. ^1H and ^{13}C NMR analysis of the terminal vinyl end group, 1,3-dichlorobutyl end group and chloromethyl branch. *Macromolecular Symposia* **1994**, *86*, 65–75.
14. (a) Percec, V.; Asgarzadeh, F., Metal-catalyzed living radical graft copolymerization of olefins initiated from the structural defects of poly(vinyl chloride). *Journal of Polymer Science Part a-Polymer Chemistry* **2001**, *39* (7), 1120–1135; (b) Bicak, N.; Ozlem, M., Graft copolymerization of butyl acrylate and 2-ethyl hexyl acrylate from labile chlorines of poly(vinyl chloride) by atom transfer radical polymerization. *Journal of Polymer Science Part a-Polymer Chemistry* **2003**, *41* (21), 3457–3462.
15. Tang, W.; Kwak, Y.; Braunecker, W.; Tsarevsky, N. V.; Coote, M. L.; Matyjaszewski, K., Understanding atom transfer radical polymerization: Effect of ligand and initiator structures on the equilibrium constants. *Journal of the American Chemical Society* **2008**, *130* (32), 10702–10713.
16. Saito, T.; Brown, S.; Chatterjee, S.; Kim, J.; Tsouris, C.; Mayes, R. T.; Kuo, L.-J.; Gill, G.; Oyola, Y.; Janke, C. J.; Dai, S., Uranium recovery from seawater: Development of fiber adsorbents prepared via atom-transfer radical polymerization. *Journal of Materials Chemistry A* **2014**, *2* (35), 14674–14681.
17. Seko, N.; Katakai, A.; Tamada, M.; Sugo, T.; Yoshii, F., Fine fibrous amidoxime adsorbent synthesized by grafting and uranium adsorption-elution cyclic test with seawater. *Separation Science and Technology* **2004**, *39* (16), 3753–3767.
18. Brown, S.; Yue, Y.; Kuo, L.-J.; Mehio, N.; Li, M.; Gill, G.; Tsouris, C.; Mayes, R. T.; Saito, T.; Dai, S., Uranium adsorbent fibers prepared by atom-transfer radical polymerization (ATRP) from poly(vinyl chloride)-*co*-chlorinated poly(vinyl chloride) (PVC-*co*-CPVC) fiber. *Ind. Eng. Chem. Res.* **2016**.
19. (a) Eloy, F.; Lenaers, R., The chemistry of amidoximes and related compounds. *Chem. Rev.* **1962**, *62*, 155–183; (b) Tian, G. X.; Teat, S. J.; Zhang, Z. Y.; Rao, L. F., Sequestering uranium from seawater: Binding strength and modes of uranyl complexes with glutarimidedioxime. *Dalton Transactions* **2012**, *41* (38), 11579–11586.
20. Flicker Byers, M.; Schneider, E., Optimization of the Passive Recovery of Uranium from Seawater. *Industrial & Engineering Chemistry Research* **2015**.
21. Schneider, E.; Sachde, D., The Cost of Recovering Uranium from Seawater by a Braided Polymer Adsorbent System. *Science & Global Security* **2013**, *21* (2), 134-163.
22. Das, S.; Liao, W. P.; Flicker Byers, M.; Tsouris, C.; Janke, C. J.; Mayes, R. T.; Schneider, E.; Kuo, L. J.; Wood, J. R.; Gill, G. A.; Dai, S., Alternative Alkaline Conditioning of Amidoxime Based Adsorbent for Uranium Extraction from Seawater. *Industrial & Engineering Chemistry Research* **2015**.
23. Flicker Byers, M.; Schneider, E. In *Sensitivity of Seawater Uranium Cost to System and Design Parameters*, GLOBAL 2015 21st International Conference & Exhibition: " Nuclear Fuel Cycle for a Low-Carbon Future", Paris, France, Paris, France, 2015.
24. Schneider, E.; Lindner, H. In *UPDATES TO THE ESTIMATED COST OF URANIUM RECOVERY FROM SEAWATER*, 19th Pacific Basin Nuclear Conference: Fulfilling the Promise of Nuclear Technology Around the Pacific Basin in the 21st Century, Vancouver, BC, Vancouver, BC, 2014.
25. Kim, J.; Tsouris, C.; Oyola, Y.; Janke, C. J.; Mayes, R. T.; Dai, S.; Gill, G.; Kuo, L.-J.; Wood, J.; Choe, K.-Y.; Schneider, E.; Lindner, H., Uptake of Uranium from Seawater by Amidoxime-Based Polymeric Adsorbent: Field Experiments, Modeling, and Updated Economic Assessment. *Industrial & Engineering Chemistry Research* **2014**, *53* (14), 6076-6083.
26. Bureau of Labor Statistics, Consumer Price Index. 2016.
27. Tamada, M.; Seko, N.; Kasai, N.; Shimizu, t., Cost Estimation of Uranium Recovery from Seawater with System of Braid Type Adsorbent. *Transactions of the Atomic Energy Society of Japan* **2006**, *5* (4), 358-363.

28. Wang, T.; Khangaonkar, T.; Long, W.; Gill, G., Development of a Kelp-Type Structure Module in a Coastal Ocean Model to Assess the Hydrodynamic Impact of Seawater Uranium Extraction Technology. *Journal of Marine Science and Engineering* **2014**, 2 (1), 81-92.
29. Whitesides, R. Process Equipment Cost Estimating by Ratio and Proportion. <http://www.pdhonline.org/courses/g127/g127content.pdf> (accessed 2 28, 2016).
30. Park, J.; Gill, G. A.; Strivens, J. E.; Kuo, L.-J.; Jeters, R. T.; Avila, A.; Wood, J. R.; Schlafer, N. J.; Janke, C. J.; Miller, E. A.; Thomas, M.; Addleman, R. S.; Bonheyo, G. T., Effect of Biofouling on the Performance of Amidoxime-Based Polymeric Uranium Adsorbents. *Industrial & Engineering Chemistry Research* **2016**.
31. Kuo, L. J.; Gill, G. A. In *Improving Adsorbent Reusability for Extraction of Uranium from Seawater*, DOE-NE Fuel Resources (Seawater Uranium Recovery) Program Meeting, College Park, MD, College Park, MD, 2015.
32. Sugo, T.; Tamada, M.; Seguchi, T.; Shimizu, T.; Uotani, M.; Kashima, R., Recovery system for uranium from seawater with fibrous adsorbent and its preliminary cost estimation. *Journal of the Atomic Energy Society of Japan* **2010**, 43 (10), 1010-1016.
33. Flicker Byers, M.; Schneider, E. In *Uranium from Seawater Cost Analysis: Recent Updates*, American Nuclear Society Annual Meeting Nuclear Power: Leading the Supply of Clean, Carbon Free Energy, New Orleans, LA, New Orleans, LA, 2016.
34. Kim, J.; Tsouris, C.; Mayes, R. T.; Oyola, Y.; Saito, T.; Janke, C. J.; Dai, S.; Schneider, E.; Sachde, D., Recovery of Uranium from Seawater: A Review of Current Status and Future Research Needs. *Separation Science and Technology* **2013**, 48 (3), 367-387.